Measurement of very-low frequency noise

Document Version:
Publisher's PDF, also known as Version of Record (includes final page, issue and volume numbers)

Please check the document version of this publication:

• A submitted manuscript is the version of the article upon submission and before peer-review. There can be important differences between the submitted version and the official published version of record. People interested in the research are advised to contact the author for the final version of the publication, or visit the DOI to the publisher's website.
• The final author version and the galley proof are versions of the publication after peer review.
• The final published version features the final layout of the paper including the volume, issue and page numbers.

[Link to publication](#)

MEASUREMENT OF
VERY-LOW FREQUENCY NOISE

JULIO LÓPEZ DE LA FUENTE

MEASUREMENT OF VERY-LOW FREQUENCY NOISE

MEASUREMENT OF
VERY-LOW FREQUENCY NOISE

DOOR

JULIO LÓPEZ DE LA FUENTE

GEBOREN TE NEGURI-GUECHO

CONTENTS

5

PREFACE

The history of electronic noise is nearly as old as the electronic devices themselves. Although in 1918 Schottky developed a quantitative study of shot noise, it was not felt necessary to develop very low noise amplifiers. At that time radio communications had little need for supersensitive receivers since the limiting noise which originated from atmospherics and statics was outside the receiver.

Similarly, until the arrival of the present age of instrumentation and control in the very low frequency range, as required in geophysics, servomechanisms, modern control systems and, most recently, in medicine, there has been no motivation for the study of very low noise amplifiers and electronic components in the very low frequency range.

All kinds of noises are almost equally annoying to the user of electronic devices, if in one way or another the noise interferes with the detection of the desired signal. Nevertheless, not all noises have the same fundamental importance. For instance, induced hum and microphonic noise can be reduced below the level of detection by means of shielding and of a careful lay-out of the design.

But other types of noise as Johnson or Nyquist noise, shot noise, $1/f$ noise and burst noise appear to be more intimately bound to the very nature of the electronic devices, and therefore they set their own noise levels. Unlike their physical sources, which may differ from type to type, these noises are random and generally stationary functions of time. But with respect to $1/f$ noise the stationarity of the process may not exist for all electronic devices.

Actually, work still remains to be done· in the design of circuits that will yield the minimum noise figure within the band of frequen- 7

cies in question and in the desired range of operating parameters. However, even more significant, much more remains to be investigated experimentally concerning the fundamental behaviour of the noise processes themselves. Naturally, such an investigation requires the use of very low noise circuits. Hence, the advance of knowledge of noise moves along the double rail track of low noise circuits and components. Consequently, noise problems will still remain with us for a long time to come.

Within the extensive area covered by the noise problems of to-day, a new look is taken at the 1/f noise and the burst noise of carbon film resistors and planar bipolar transistors at very low frequencies.

VERY-LOW FREQUENCY NOISE

Introduction

The very word "noise" is something disturbing, because of the lack
of intelligibility it carries within itself rather than its sound
effect. Noise is everywhere in nature although frequently one can-
not hear it, since its scientific meaning goes far beyond its prim-
itive sense of an unpleasant acoustical wave. Thus the word "noise"
is taken to mean generally a cause of disturbance in no matter what
field of interest.

The ancient discovery of light bodies being attracted by a bar of
amber softly rubbed with a cloth is attributed to the philosopher
Thales of Milete[1-1] in 600 B.C. This property was named "electrici-
ty", since the amber had the Greek name of "ἤλεκτρον". Many centu-
ries later, in 1891, George J. Stoney[1-2] was to use the term "elec-
tron" for designating the elementary negative particle, which since
then has become an instrument of energy and information inseparable
from mankind.

But already in 1828 R.Brown[1-3] observed that particles of polen or
dust suspended in a liquid showed random motion. Almost a century
later it was predicted that a similar phenomenon with electrons would
occur in an electrical conductor, yielding a spontaneous generation
of a random E.M.F. across the terminals of the conductor.

Although man has learned to control the electron for its multiple
purposes, his control is limited. The limitation comes about from
the electron being affected by the surroundings in which it is han-
dled. The medium leads the electron to behave variously and mani-
foldly, the behaviours appearing to us as disturbances or as elec-
tronic noise.

The first striking property of noise is to give a unique observation each time the phenomenon is contemplated. Thus, the movement of the electrons in a conductor gives rise, among other effects, to a random terminal voltage which determines the ultimate sensivity of information transmitted through the conductor. Therefore, man has always fought against noise as a cause of disturbance with a better knowledge of its origin and energy content, the aim being to decrease its effects.

In the following pages we will be concerned mainly with certain types of electronic noise measured by an appropriate detecting system. The specific physical origin or possible sources of noise will be treated in so far as their consideration leads to the design of a low-noise measuring system for random phenomena and helps to obtain new insights into the nature of noise in the very low frequency range. We will measure the noise energy spectrum and determine certain behaviour properties of some electronic components.

1. Stationarity and ergodicity of random phenomena

In order to study the noise properties of devices and the noise behaviour of circuits we need essentially a certain amount of mathematical background on probability, statistical and Fourier analysis.

Our measurements involving noise sources will give a large amount of data from a physical phenomenon, which when observed can be classified under the concept of random and not deterministic phenomena.

When the relation between cause and effect of a physical behaviour is expressible by an explicit mathematical relationship, the phenomenon is called deterministic and its behaviour may be periodical or transient. On the contrary, a phenomenological behaviour is called random when no explicit mathematical expression can be found for the cause-effect relationship, because two observations of the phenomenon may not give the same value. Hence, any given observation represents only one of the many possible results which might occur.

The collection of all possible observations of the random phenomenon is known as a stochastic or random process, while a group of observations constitute an ensemble of the process.

It is here, in manipulating the random data of the ensemble that statistics has become the reasoning instrument since an individual factor has little influence on the phenomenological behaviour which is subjected to the overwhelming presence of a multitude. This fact is the basis of the law of the large number of observations.

In electricity it is synonymous to speak about random processes x(t) or fluctuating electrons, namely electrical noise. Hence the terms "fluctuation" and "randomness" refer to related physical quantities.

One important property of statistical techniques is that every parameter is considered with an average value and with the fluctuations from this average. The fluctuation around an average value:

$$\mu = \lim_{N \to \infty} \frac{1}{N} \sum_{k=1}^{N} x(t_k) \tag{1.1}$$

is best described by the probability density distribution P(x), which prescribes that for any instant of time the chance that x(t) is inside the interval (x, x + dx) equals P(x)dx. Thus, the probabilistic knowledge of the instantaneous value of the phenomenon is represented by some probability distribution type such as the binomical, Poisson or Gaussian.

As the interval τ between two individual observations of the random process increases, the averaged product correlates the general dependence of the data values into a function called the autocorrelation function:

$$R(\tau) = \lim_{N \to \infty} \frac{1}{N} \sum_{k=1}^{N} x(t_k) \, x(t_k + \tau) \tag{1.2}$$

For deterministic data, R(τ) persists for all displacement values of τ. But for a random process the autocorrelation function tends to zero as τ tends to infinity, and is a bounded function in the time domain. The Fourier transform of the autocorrelation function yields the spectral power density function of the random process and contains significant relations with the characteristic behaviour of the measuring system (see chapter 2).

Nevertheless, the observation of the power spectrum in itself gives little information concerning the identity of the source of fluctuations, since many different disturbing sources may have the same power density distribution.

When the statistical properties remain the same for ever, the process is called stationary. Now, in practice the random process is observed during a finite interval T during which we obtain a certain average μ_T and an autocorrelation function $R_T(\tau)$. When μ_T and $R_T(\tau)$ tend to have a constant value as the observation time T over which they are computed is increased, the process is said to be stationary in practice. When the statistical properties do not remain the same for ever, the process is called non-stationary. But, when the statistical properties of a process are changing sufficiently slowly in order not to show appreciable change during the period T of any one observation of the phenomenon, the process is named quasi-stationary.

The problem of determining the conditions under which averages of a stochastic process as observed on one sample can be ultimately identified with corresponding averages on an ensemble of samples, leads to the consideration of an ergodic process. In general, a stochastic process is said to be ergodic, if the time-averaged mean value of a sample (equation (1.1)) and the time-averaged autocorrelation function of that sample (equation (1.2)), as well as other statistical properties, are equal to their corresponding ensemble averaged value $\mu_x(t)$, $R_x(t,t + \tau)$,..... where:

$$\mu_x(t) = \lim_{N \to \infty} \frac{1}{N} \sum_{k=1}^{N} x_k(t) \tag{1.3}$$

and

$$R_x(t,t + \tau) = \lim_{N \to \infty} \frac{1}{N} \sum_{k=1}^{N} x_k(t)\, x_k(t + \tau) \tag{1.4}$$

Thus, only stationary random processes can be ergodic. In practice, most of the physical phenomena that produce stationary random data correspond to ergodic processes[1-4]. Nevertheless, we shall come across some non-ergodic processes.

2. Electrical noise. Its power density spectrum

Let us consider now the fluctuation of electrons in an arbitrary
body or the "electrical noise" as it is more commonly called.

Johnson and Nyquist showed that the fluctuation of electrons has to
be considered as an important factor when designing sensitive elec-
trical networks. So important, in fact, that the level of fluctua-
tion determines the limit of sensitivity. Apparently we have reached
a dead end. But there is a way out, which consists in exploring back-
wards the possible paths that end in such a fluctuating situation.
These paths lead to the atomistic character of a particular electri-
cal conduction mechanism. Sometimes, when we are not able to reach
the end of the path of exploration we shall study the energy contents
of the fluctuations while regarding their possible noise sources.

Surely enough, many of these paths have crossings and even sometimes
run parallel, indicating the interference and simultaneous presence
of different causes. Hence, an even larger complexity is introduced
then in identifying the physical source. We have to admit that the
explanation of noise appears to be paradoxal to-day, since so many
different theories are proposed for any one type of noise. But it is
hoped that eventually it will be possible to follow a unique or at
least the shortest path towards the source within this labyrinth of
theories.

Nyquist[1-5] showed that a resistor of R ohms at a temperature of T $^\circ$K
which is in thermal equilibrium with its surroundings, develops at
its terminals and in an effective bandwidth Δf an open circuit noise
voltage e_n whose rms value is given by:

$$e_n = \sqrt{4kTR\Delta f} \qquad\qquad\qquad (1.5)$$

where k is Boltzmann's constant.

Thermal noise is caused by the thermal agitation of electrons in con-
ductors and semi-conductors. Its power density may be determined from
thermodynamics and statistical mechanics. Now, thermodynamic entropy
is a measure of disorder or of the uncertainty about the microscopic 13

state of a thermodynamic system. Then, from the point of view of energy generated and heat dissipated a physical system where the entropy is maintained at a constant level, is said to be randomly stationary[1-6]. Such is the case for the thermal noise of an element being measured at a constant temperature.

But Nyquist's formula applies only to thermal equilibrium conditions, and electrical devices do not operate in such conditions, since a current usually flows through them. This current is the basis of a noise current source.

In a vacuum diode the noise owing to its d.c. anode current is known as shot noise, which is the result of fluctuations in the instantaneous number of electrons in transit caused by the random electron emission of the cathode. The mean square value of shot-noise current $\overline{i_n^2}$ in a saturated diode where I_d is the direct current of the diode, -q is the electronic charge, and Δf is the effective noise bandwidth under consideration, is given by[1-7]:

$$\overline{i_n^2} = 2 \ q \ I_d \ \Delta f \qquad (1.6)$$

In (1.6) the frequency of measurement must be low enough to avoid transit-time effects and high enough to avoid low-frequency effects covered in the following sections.

Thermal noise and shot noise, as given by equations (1.5) and (1.6), are independent of the measuring frequency and so have a flat power density spectrum $S(f)$ known as "white spectrum". Nevertheless, active and passive devices carrying a current show a noise power density level higher than the theoretical values given by (1.5) and (1.6), and their total power density distribution is of the type given by Fig. 1.1.

Three distinct regions are shown in Fig. 1.1. (i) On the right is the high frequency region, where $S(f)$ increases proportionally to f^α, with $\alpha \simeq 2$, from a frequency value f_2 which is usually in the MHz range. (ii) The medium frequency region corresponds to the white noise, where $S(f)$ is constant down to some frequency value f_1. The actual value of f_1 depends on the type of device in question, the

14
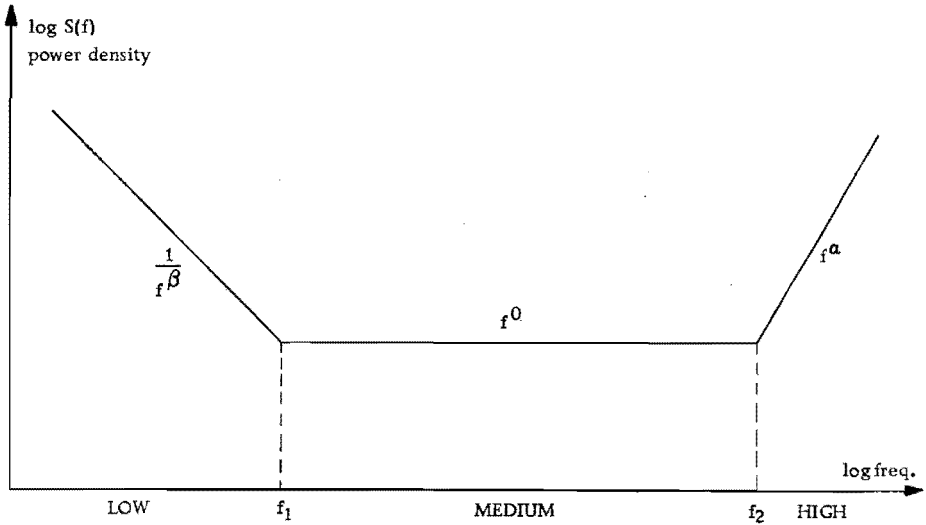
Fig. 1.1   Noise power density spectrum

individual sample, and its operating mode. Thus, for a low-noise vacuum tube f_1 is around 1 kHz, while for a transistor it can be 50 Hz, both devices operating at 1 mA d.c. current. (iii) The third region refers to the low and very low frequencies, following a law proportional to $f^{-\beta}$; with $0 \le \beta \le 2$.

It is in this last region that lies our main interest.

3. Low-frequency current noise

(A) Flicker noise

The term "current noise" is meant to include all noise types other than thermal noise (1.5) and shot noise (1.6) which appear in a device carrying a current. Although the physical cause of the additional noise level is not clear, many experiments have shown that the noise spectrum at low frequencies has the following type of law:

$$S(f) = K \frac{I^a}{f^\beta} \tag{1.7}$$

where I is the d.c. current, $a \simeq 2$ and $0 < \beta \le 2$. The coefficient K is an empirical factor involving the geometry[1-8] and material of the 15

device and depending weakly on the temperature in a way not precise-
ly known[1-9].

When this phenomenon was first discovered in vacuum tubes[1-10], show-
ing a value of β close to unity, it was called "flicker noise". To
other devices with similar spectra other names are given such as
"1/f noise", "excess noise", "semi-conductor noise", "low frequency
noise", "contact noise" and "pink noise".

Flicker noise seems to appear everywhere. Apart from vacuum tubes it
may be found in resistors[1-11], thin carbon films[1-12], carbon micro-
phones[1-13], thermistors[1-14], bipolar transistors[1-15] and semi-con-
ductor diodes, photoconductors[1-16], quartz crystal oscillators[1-17],
and in field-effect transistors[1-18]. We see that most of the materi-
als in which 1/f noise arises can on one ground or another be clas-
sified as semi-conductors. Our main interest will cover resistors
and transistors. Although the general case is for $\beta \simeq 1$ in equation
(1.7), there are some interesting cases in which β is greater than
unity.

From the consideration of the noise power in a frequency band from
f_1 to f_2 it can be seen that

$$\int_{f_1}^{f_2} S(f)df = \frac{K}{1-\beta} f^{1-\beta}\bigg|_{f_1}^{f_2} \qquad (1.8)$$

yielding infinite mean power when β is ≤ 1 and f_2 extends to infi-
nity or when β is ≥ 1 and f_1 extends to zero frequency. Therefore,
such a law as given by equation (1.7) cannot hold for all frequen-
cies, and it is then necessary that β becomes smaller than one at
some very low frequency and is larger than one at high frequencies.
But up to the present no low frequency has been found in experiments
below which the value of β in (1.7) decreases. (Note).

(Note). A possible way out of this difficulty is presented by Mala-
kof[1-19], who seems to have been the first to point out the possibili-
ty of flicker noise being non-stationary with stationary increments,
i.e. flicker noise is quasi-stationary.

In order to encompass these considerations as well as the experimental evidence, the low frequency region of Fig. 1.1 is developed into the representation of Fig. 1.2. Thus, the importance of the parameter β is emphasised.
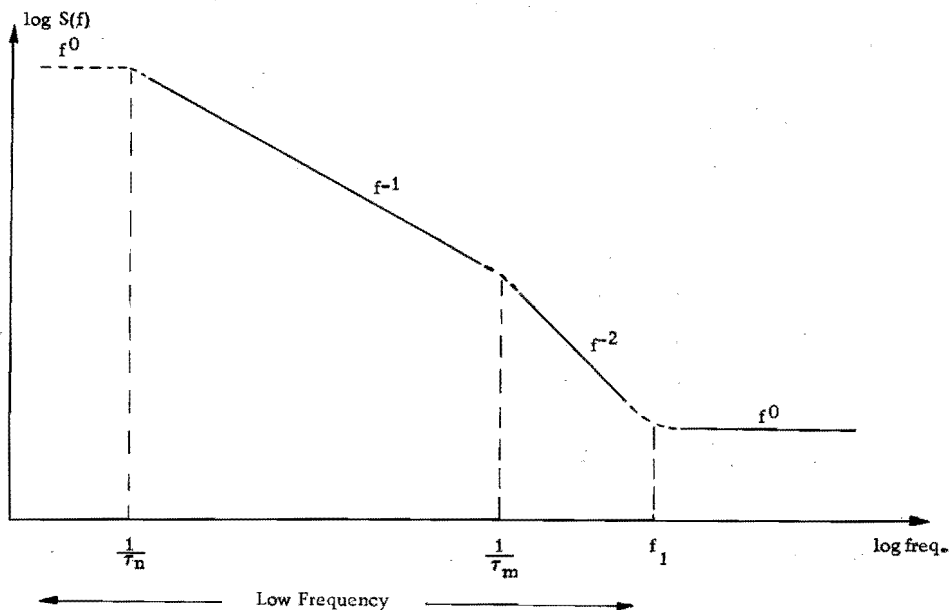
Fig. 1.2   Low-frequency noise power density spectrum

Indeed, after the first work of Bernamont[1-11] several investigators followed his line of study. Meyer and Thiede investigated thin carbon films confirming the value of a=2 in equation (1.7) but obtaining a variation in β, $1 \leq \beta \leq 2$.

It is known that good vacuum diode tubes with a tungsten filament have a flat spectrum down to about 30 Hz and then start to increase as f^{-2} or even sometimes as f^{-3} as the frequency decreases[1-20, 1-21].
An experimental f^{-2} may be understood as pertinent to a spectrum law:

$$S(f) = K \frac{\tau}{1 + (\omega\tau)^2} \tag{1.9}$$

where τ is the mean lifetime of a single event which affects the conductivity of the sample, ωτ is to be considered sufficiently   17

large, K is a constant, and ω is the angular frequency. If the
transit time of an electron from cathode to anode in a vacuum diode
or similarly the generation-recombination time of an electron in a
semi-conductor diode, is considered as the lifetime of the single
event, equation (1.9) represents the noise spectrum of shot noise.
But, in case a continuous distribution of τ is considered with a
probability distribution of τ proportional to $1/\tau$ between limits
τ_m and τ_n, an f^{-1} law results as a sum of all possible spectra of
type (1.9) in a certain frequency range.

It may occur that of the spectrum components of type (1.9) some are
much larger in magnitude than the other ones. Then, the whole spec-
trum of Fig. 1.2 can be represented by a sum of a uniform component,
an f^{-1} component and one or several components $\tau/(1 + (\omega\tau)^2)$, yield-
ing the spectrum relation[1-22]:

$$S(f) = A + \frac{B}{\omega} + \frac{C\tau}{1 + (\omega\tau)^2} \tag{1.10}$$

In fact, the spectrum relation (1.10) has been verified experimen-
tally in semi-conductors as germanium filaments, p-n junctions and
transistors, as well as in vacuum tubes and mos transistors very re-
cently. A summary of this evidence follows now according to the
times of their discovery.

Noise was studied in an n-type germanium filament[1-23] in the spec-
tral range 1 kHz to 10 MHz. The spectrum followed a curve close to
(1.10) with a lifetime τ of 1 µsec. Other authors[1-24] have found,
in the lower frequency range of 10 Hz to 100 kHz, that germanium
filaments may show a clear change in S(f) from f^{-2} to f^{-1} as the
frequncy decreases. The spectrum appeared to follow equation (1.10)
and some samples showed "bumps" around 300 Hz, where a shot-noise
component was assumed to exceed the f^{-1} component. Similar results
have been reported[1-25] for a narrow germanium p-n junction which was
forward biased. The spectrum in the range of 100 Hz to 20 kHz may be
represented by (1.10), so that a peak or bump is also present when
the f^{-1} component is subtracted.

18 More recently, noise power of different planar transistor types with-

in the range of 1 Hz to 10 kHz showed a spectrum law $f^{-\beta}$ with 0.96 < β < 1.23[1-26]. Certain transistor types at 100 Hz and lower frequency values exhibited an additional noise component of the form (1.9). This last component could not be attributed to shot effect since lifetimes of msec and longer were required for explaining the spectrum.

Recently, the anomaly in the flicker noise spectrum, with $f^{-\frac{3}{2}}$ between 10 Hz and 10 kHz, was also observed in vacuum tubes with oxide cathodes[1-21]. The anomaly appeared in the range of 100 Hz to 1 kHz and was caused by an additional component in the noise spectrum which varied according to $(1 + (\omega\tau)^2)^{-1}$. In mos transistors[1-27] a spectrum bump of extra current noise at 5 kHz was found in addition to the f^{-1} component for the total current noise spectrum, following equation (1.10) in the frequency range of 20 Hz to 40 kHz.

(B) Burst Noise

While flicker noise is ubiquitous, burst noise seems to be sporadic in nature. The latter is somehow associated with the former.

In addition to flicker noise, irregularly distributed large pulses of low frequency, sometimes called "bursts", often appear in materials carrying a current. These bursts produce an audible effect in radio receivers described as crackles. In the noise power density spectrum the anomalies these bursts produce may often be represented by a specific relaxation time τ giving a relation similar to equation (1.9).

Burst noise has been found in resistors and in semi-conductor devices. The description of the phenomenon is a complex task, as may be seen in the following exposition, owing to the diversity of devices and their operating conditions under which burst noise was observed. Campbell and Chipman[1-28] as well as many others[1-14, 1-29, 1-30] observed bursts of irregular shape as abnormal fluctuations in the records of current noise from carbon resistors. The bursts did not necessarily occur at a high mean level of current, since narrow current paths exist in carbon resistors where on several spots high current densities may occur.

A more defined form of burst noise with a step waveform, similar to an unsymmetrical random telegraph signal, suggesting temporal transition between two states of conduction appears frequently in semiconductor devices.

In fact, Pay[1-31] found that a point-contact gemanium diode at 1 mA reverse current gave an almost regular rectangular noise wave of 500 Hz. He related the phenomenon to the Zener effect, a breakdown by an avalanche mechanism.

Planar and mesa structure silicon diodes were studied at the much lower reverse current of 50 µA[1-32]. Flat-topped current pulses of 30 µA and 17 µA at approximately 20 kHz were observed before reaching the avalanche situation. The bursts were thought to be associated with microplasmas and had the peculiar feature that as the reversed current was increased (1 - 300 µA), the interval between pulses decreased, until finally the microplasma saturated and no "off" pulses were observed.

In some devices, as in low voltage reverse biased germanium junctions[1-33], the current-noise wave consists primarily of a square wave with steps of 10^{-8} A in amplitude, which are much smaller than the typical microplasma pulses described above. The pulse amplitude and the switching rate changed slowly with the reverse voltage, but in a different manner than for the microplasmas. The measured time duration of the positive and negative pulses suggested a Poisson probability distribution, while the variation of the pulse height with temperature indicated that possibly random thermal fluctuations caused on-off switching of a conduction path. The physical cause of such a burst-noise phenomenon was believed to be not an avalanche breakdown but the surface effects.

Bistable current fluctuations have been found also in the reverse-biased emitter-to-base junction of p-n-p germanium diffusion transistors, within the range of low reverse voltages far below the breakdown situation[1-34]. Increasing the reversed bias had no influence on the pulse rate, which followed a Poisson distribution; but it caused a linear increase in the pulse height (which was of the order of 20 nA) until a saturation level of the pulses was reached

20

around 10 V. The pulse rate increased with temperature and the power density spectrum followed a clear f^{-2} law over two decades (20 kHz to 200 Hz) changing to an f^{-1} spectrum below 200 Hz.

More extensive work has been done on the burst noise of transistors in the forward mode of operation[1-35], [1-37]. Among the 40 planar transistors tested, 23 had burst noise, while only one in 25 transistors of diffusion or mesa structure showed bursts. The bursts appeared as a random telegraph signal with a magnitude depending on the temperature, the base resistor, and the biasing current (20 - 200 μA). The pulse lenghts had nearly a Poisson probability distribution and extended from some hunders of microseconds to some minutes. We have also observed this type of burst noise in transistors and have found pulses as long as thirteen minutes. Some transistors present three or even four levels of pulse height which are considered to be independent series. According to the authors[1-37], within the frequency range of 10^{-2} Hz to 10 kHz and for the current levels mentioned above, a spectrum f^{-1} was verified. Unfortunately no indication was given concerning the deviation from a substantially 1/f dependence.

In order to separate surface effects from bulk effects, gate-controlled diodes and transistors have been studied[1-38]. Burst noise, both gate-voltage dependent and independent, was observed. An advantage of this structure is that it becomes possible to use the gate electrode, which is placed on the base-emitter junction, to turn on and off the burst-noise source. In the frequency range of 20 Hz to 40 kHz, the diodes showed noise spectra f^{-2} down to 1 kHz and a change to f^{-1} at 40 Hz, while the transistors had an $f^{-\beta}$ spectrum with $\beta \sim \frac{3}{2}$ down to 100 Hz, and then β became smaller than unity.

Under the name of "popcorn noise" has appeared in literature a low-frequency (10 Hz to 40 kHz) step fluctuation noise. It is most often encountered in the integrated operational amplifiers and is probably due to the integrated planar transistors which jitter erratically between two or more values of h_{fe}[1-39], [1-40]. The step am-

plitude at the input of the device may reach a level of 50 µV or an equivalent input noise current of 200 pA.

Burst noise certainly does not occur or at least is not detected in each device made by a given process nor even from the same wafer. Nevertheless, from experimental evidence[1-35], [1-41] there is a good indication that the general planar technology introduces a substantial basis for the appearance of burst noise in semi-conductor devices.

Although the information of sections 3 and 4 is overwhelming, we may note the following. Some unified considerations can be made if the exponent value β of equation (1.7) and the shape of the noise power spectrum curve are taken as the basis of comparison in the noise behaviour of the different components and of the operating conditions.

Therefore, we intend to investigate the behaviour of the parameter β as well as the intensity of the flicker-noise spectrum in resistors and transistors.

With respect to the burst noise, since it has a well-defined waveform in transistors, a mathematical analysis of its spectrum will be made and compared with actual noise power measurements. Assuming a relationship between the flicker and burst noise components at very low frequencies, we will arrive at a picture close to the actual noise power spectrum curve.
But let us first establish in the following chapter the theoretical basis required for the construction of a measuring channel of power spectra.

THE MEASUREMENT OF NOISE POWER SPECTRA

1. The measurement of a random process

It is our intention to measure the power spectra of some stochastic
or random processes and we shall see that it can be done by a hy-
brid system that combines analogue and digital techniques. The
reasons for measuring power spectra as a parameter that gives in-
formation about noise may be understood from the following consid-
erations.

When considering noise currents or voltages, f(t), very little in-
formation about the behaviour of f(t) is obtained from the knowl-
edge of an instantaneous value, because instantaneous values may
differ much in magnitude and may also be lacking in reproducibili-
ty. Neither it is possible to predict the past or the future be-
haviour of f(t) from only the instantaneous values observed during
an interval T. However, averaged functions of f(t) over a long
time T can lead to a more extensive knowledge of the signal's be-
haviour.

For a stationary random process, f(t), the average value over the
past, present, and future is its d.c. component value $\overline{f(t)}$. Now,
the average value of the fluctuations of f(t) around $\overline{f(t)}$ is zero
but their variance, i.e. the averaged squares of the differences
between $\overline{f(t)}$ and its instantaneous values f(t), is a positive
quantity:

$$\overline{\left(f(t) - \overline{f(t)} \right)^2} = \overline{\phi(t)^2} = \lim_{T \to \infty} \frac{1}{2T} \int_{-T}^{T} \phi(t)^2 dt \qquad (2.1)$$

If $\phi(t)$ is the voltage across a resistor of 1Ω or the current flow-
ing through the load of 1Ω, the numerical value of $\phi(t)^2$ is equal
to that of the power dissipated by the voltage or the current in

23

the resistor load. Therefore, $\phi(t)^2$ is a relevant feature of the random generating process $f(t)$ and it is customary to speak about $\phi(t)^2$ as being a power quantity, even if its dimension is not that of a power.

In practice, $\phi(t)$ it is a noise signal of small magnitude and an amplifier is needed to increase its level before we can manipulate it. We would also like to have a unique input-output correspondence of the noise signals that will allow true interpretation of the input data. The simplest choice is to use a linear amplifier.

Let us apply a sinusoidal voltage $A_i \cdot \exp j\omega t$ to the input of the linear amplifier and obtain an output voltage $A_o \cdot \exp j(\omega t + \theta)$; here A_o and A_i are real numbers. Then the transfer function of the linear system is defined as:

$$H(\omega) = A_o e^{j(\omega t + \theta)} \Big/ A_i e^{j\omega t} = A_o/A_i \cdot e^{j\theta} \qquad (2.2)$$

where A_o/A_i is known as the gain factor of the system at the frequancy ω of consideration, and θ is called the phase angle. It can be proved [2-1] that:

$$H(\omega) = \int_{-\infty}^{\infty} h(\tau) e^{-j\omega \tau} d\tau \qquad (2.3)$$

where $h(\tau)$ is the response of the system initally at rest to a unit impulse at $\tau=0$. Now, the output $\phi_o(t)$ resulting from an input signal $\phi_i(t)$ t$ to a linear system can be written as a convolution or superposition integral:

$$\phi_o(t) = \int_{-\infty}^{\infty} \phi_i(t) h(t-\tau) d\tau = \int_{-\infty}^{\infty} h(\tau) \phi_i(t-\tau) d\tau \qquad (2.4)$$

where $h(\tau)$ appears as the weighting function of a linear system which, by exploring the past of the input function, with its unit-impulse response, supplies the output function.

However, for a random process we are interested statistically on-
24 ly in average values not of the time functions themselves but in

the time averaged quadratic values. Let us first consider the autocorrelation function $\overline{\Phi}(\tau)$, which is defined as:

$$\overline{\Phi}(\tau) = \overline{\phi(t)\ \phi(t+\tau)} = \lim_{T\to\infty} \frac{1}{2T} \int_{-T}^{T} \phi(t)\ \phi(t+\tau)dt \qquad (2.5)$$

From (2.5) the power as given by equation (2.1) can be obtained by letting $\tau \to 0$, i.e. $\overline{\Phi}(o)$. Now, the integral $\int_{0}^{\infty} |\overline{\Phi}(\tau)|d\tau$ exists. Therefore, the Fourier transform of $\overline{\Phi}(\tau)$ can be taken.

When we consider at the input of a linear system with transfer function $H(\omega)$ the autocorrelation function $\overline{\Phi}_i(t)$ of the stationary random process, we may write for the autocorrelation function $\overline{\Phi}_o(t)$ at the output [2-2] :

$$\overline{\Phi}_o(\tau) = \iint_{-\infty}^{\infty} h(t)\ h(\eta)\ \overline{\Phi}_i(t + \tau - \eta)\ dtd\eta \qquad (2.6)$$

Expression (2.6) enables us to obtain, entirely from operations in the time domain, the output autocorrelation function from an input autocorrelation function and the weighting function of the system. If we apply a Fourier transform to (2.6), having made the change of variables $\mu = \tau + t - \eta$, we may write:

$$\frac{1}{2\pi} \int_{-\infty}^{\infty} \overline{\Phi}_o(\tau)e^{-j\omega\tau}d\tau = \int_{-\infty}^{\infty} h(\eta)e^{-j\omega\eta}d\eta \int_{-\infty}^{\infty} h(t)e^{j\omega t}dt \quad \times$$

$$\frac{1}{2\pi} \int_{-\infty}^{\infty} \overline{\Phi}_i(\mu)e^{-j\omega\mu}d\mu$$

which by the Wiener-Khintchine theorem yields:

$$S_o(\omega) = H(\omega)\ H^*(\omega)\ S_i(\omega) = |H(\omega)|^2\ S_i(\omega) \qquad (2.7)$$

where $S_o(\omega)$ and $S_i(\omega)$ represent the power density spectrum of the output and input of the system, respectively. $S(\omega)d\omega$ is the amount of average power present within an infinitesimal bandwidth $d\omega$ centered at a specific frequency ω.

Now, since $\overline{\Phi}(\tau)$ and $S(\omega)$ are a pair of reciprocal relations in a Fourier transform, we have for $\tau\to 0$: $\overline{\Phi}(o) = \int_{-\infty}^{\infty} S(\omega)d\omega$, which is the 25

total power. Then, integrating both sides of equation (2.7) and having replaced $\bar{\Phi}_o(o)$ by its equivalent through equations (2.5) and (2.1), we obtain for the output power:

$$\overline{\phi_o(t)^2} = \bar{\Phi}_o(o) = \int_{-\infty}^{\infty} S_o(\omega)d\omega = \int_{-\infty}^{\infty} |H(\omega)|^2 S_i(\omega)d\omega \qquad (2.8)$$

where $\phi_o(t)$ corresponds with the instantaneous output fluctuations of the linear system. The right-hand side of equation (2.8) represents a spectrum in which $|H(\omega)|^2$ appears as a weighting factor of the input power density spectrum. Therefore, if the linear system is considered to be a narrow filter with bandwidth $\Delta\omega$ and centered at ω_o it is possible to scan the total power of the random process into its power frequency components. In fact. (2.8) yields:

$$\overline{\phi_o(t)^2} = \int_{\omega_o - \frac{\Delta\omega}{2}}^{\omega_o + \frac{\Delta\omega}{2}} |H(\omega)|^2 S_i(\omega)d\omega \qquad (2.9)$$

and assuming that for a stationary random process $S_i(\omega)$ corresponds to a smooth spectrum, we may write (2.9) as:

$$\overline{\phi_o(t)^2} = S_i(\omega_o) \int_{\omega_o - \frac{\Delta\omega}{2}}^{\omega_o + \frac{\Delta\omega}{2}} |H(\omega)|^2 d\omega \qquad (2.10)$$

so that $S_i(\omega_o)$ may be obtained from a measurement of $\overline{\phi_o(t)^2}$ using that particular frequency filter, provided that the integral on the right-hand side is known. This integral represents the area of the power spectral window corresponding with the filter.

Thus, equation (2.10) provides a simple relation that allows us to calculate the spot power density of the input random stationary process $f(t)$ from averaged quadratic fluctuations at the output of the linear system and the integral of the squared gain factor of the system, having avoided every complication by phase. As ω_o is varied, the whole power density spectrum is obtained.

In practice, owing to the finite observation time T of the random process, estimates are made on average values by observing the random process during a sufficiently long time T.

26

2. The measuring system

The application of a filter in equation (2.10) demands two requirements:

I   : in the frequency domain the bandwidth $\Delta\omega$ must be sufficiently small with respect to the smooth region of the power spectrum being considered.

II : in the time domain, the unit-impulse response $h(\tau)$ of the filter requires a certain time τ_m in order to vansih. This time must be smaller than the observation time T for obtaining a complete response of the system to the input.

Therefore, the system's behaviour of such a selective filter centered at ω_o has the following expression:

In the frequency domain:

$H(\omega) =/= 0$ within $\omega_o \pm \Delta\omega/2$

$\quad = 0$ elsewhere

In the time domain:

$h(\tau) =/= 0$ for $0 < |\tau| \leq \tau_m < T$

$\quad = 0$ for $|\tau| > \tau_m$

Now, the evaluation of $\overline{\phi_o(t)^2}$ in (2.10) is obtained by integrating over an infinite time. But in practice, for a stationary random process an approximate value $\overline{\phi_{oT}(t)^2}$ is obtained with a certain statistical accuracy ε (see section 5) by integrating over a sufficiently long time T.

Therefore, at a particular spot frequency value ω_o, having measured during time T, we obtain for equation (2.10):

$$S_{iT}(\omega_o) = \overline{\phi_{oT}(t)^2}/k\Delta\omega \qquad (2.11)$$

where $k\Delta\omega$ is the area of the power spectral window of the filter.

Fig. 2.1 shows a block diagram of the measuring system for power

$\phi_{iT}(t)$ $\qquad$ $\phi_{iT}(t)*h(\tau) = \phi_{oT}(t)$ $\qquad$ $\frac{1}{T}\int_o^T \phi_{oT}(t)^2\,dt = \Phi_{oT}(o)$

Noise source		$h(\tau)$ Filter , $\Delta\omega$ $H(\omega)$		Integrating-Averaging Power Instrument	
	a		b		c
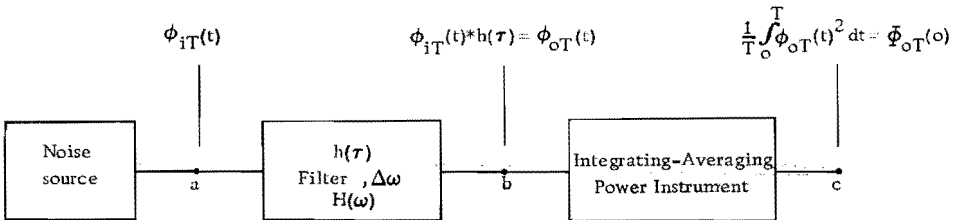
Fig. 2.1 Block diagram of the measuring system.   **27**

spectra of a noise source by using a selective frequency filter and an integrating-averaging power instrument. In fact, let $\phi_{iT}(t)$ represent the fluctuations of the noise source around its average value during an interval of time T. Then, in the time domain at point **b** in Fig. 2.1 the convolution of $\phi_{iT}(t)$ and $h(\tau)$ yields $\phi_{oT}(t)$ through equation (2.4), while at point **c** the output represents $^{1}/T \cdot \int_{o}^{T} \overline{\phi_{oT}(t)^2} dt$ which corresponds to an autocorrelation value $\underline{\Phi}_{oT}(o)$ through equation (2.5), an approximation to the exact value $\underline{\Phi}_{oT \to \infty}(o)$; and dividing by $k\Delta\omega$, we obtain $S_{iT}(\omega)$.

It is seen from the above considerations that the lay-out of Fig. 2.1 is sufficient for resolving equation (2.11).

3. Low Q window

In practice, a filter with a flat response and a sharp cut-off is only realisable by a complex circuit. A narrow-band filter has a large τ_m value while a filter with a small τ_m introduces an undesired effect upon the spectral window owing to the appearance of large sidelobes. Blackman and Tukey [2-3] have shown that a filter with a theoretical square lag-window $h(\tau)$ gives in the output power a first sidelobe in the spectral window as high as 20% of the mainlobe and it is negative (Fig. 2.2). Measuring noise through such a filter, at its output we would also obtain contributions to the noise by frequencies far apart from the central frequency ω_o.
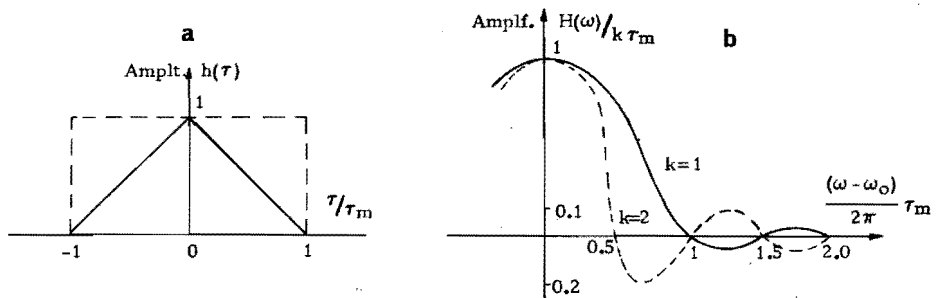
Fig. 2.2   a) Lag window.
*   b) Spectral window.*

As the shape of the lag window is changed into a triangular shape, the amplitudes of the sidelobes in the spectral window are reduced very rapidly, being at most 1% or 2% of the height of the mainlobe. Thus, the main power contribution is now by far restricted to a much smaller region around ω_o.

Special windows have been designed, such as the "hamming" and "hanning" windows, with the aim of producing very small sidelobes. But Blackman [2-4] points out that any special window cannot eliminate the need for prewhitening and the rejection of filtrations, while good prewhitening and rejection filtration can eliminate the use of special windows. Therefore, a logical and practical compromise may be reached by the design of a wide bell-shaped filter, namely, a low Q filter.

Low Q filters tend to be bell-shaped. But their rejection filtration is not so good since their frequency characteristic curve $H(\omega)$ has non-zero amplitude tails that extend over some decades of the frequency spectrum. Therefore, very large signals outside the pass-band are not well rejected, and so leak through the tails of the filter and give an extra power contribution at the output of the system.

Even when the above large signals are not present in the measurement in question, and a white noise spectrum is to be measured, one further consideration has to be made. The output power at c in Fig. 2.1 is then proportional to the total area under the bell-shaped curve $|H(\omega)|^2$ of the filter. At low spot frequency values of ω_o, the actual bandwidth is necessarily small and a situation may be reached in which the area under the two side-tails of the bell curve is considerable with respect to the central area. Then, an appreciable error results in the output power measurement localised at ω_o. Consequently, a high-pass and a low-pass filter section must be added to the low-Q bell-shaped filter, if an improvement is to be expected from the measuring system. Thus, the block of $H(\omega)$ corresponds in practice to Fig. 2.3.

Since the spectrum range under consideration is the very-low frequency band 10^{-2} Hz to 20 Hz, it seems convenient that the low-
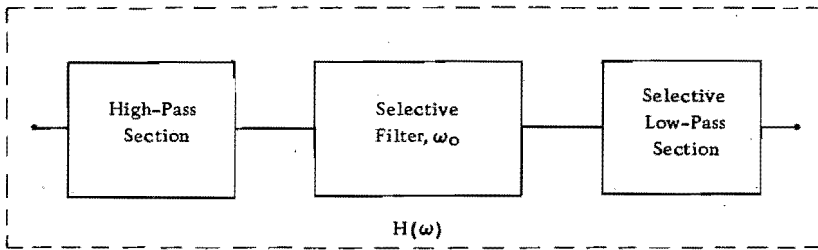
Fig. 2.3   Block diagram of the filter, H(ω).

pass section be selective in order to obtain a sharp cut-off re-
sponse on the high-frequency side tail. The high-pass section is
realisable by a prewhitening filter placed in front of the selec-
tive filter, as may be seen in the following section.

In the power density spectrum representation a logarithmic scale
is foreseen to be convenient, and equally spaced value of log ω_o
are desired. This leads us to choose the ω_o values per decade as
follows:

k. 1, k.$\sqrt[3]{10}$, k.$\left[\sqrt[3]{10}\right]^2$ or ω_o: 1, 2.15, 4.64 per decade.

By this choice we obtain 11 points in the power spectrum of in-
terest so that a well-approximated curve can be drawn.

4. Prewhitening

Prewhitening consists in filtering the data before their analysis
is started, in order to remove the possible excessive influence
of spectral peaks and thus obtain a smooth power spectrum at the
output. Consequently, any interference between different compo-
nents is minimised and a picture closer to the real spectrum ap-
pears after recolouring.

The objective of prewhitening is to minimise the total mean square
error of an estimated value [2-5] and to decrease considerably the
peak of the spectrum near the d.c. component. At the same time,
saturation by this part of the spectrum is avoided in the ampli-
fiers needed for the measuring system, and a flat or a white noise
spectrum is analysed at the output. Therefore, prewhitening should
30   be done as early as possible in the system so that the selective

filter operates under equivalent power relations independently of the spot frequency value ω_o under consideration.

The main difficulty lies in the necessity of knowing "a priori" the shape of the input power spectrum to be analysed and that this shape may require highly flexible filters which are often difficult to design.

Fortunately, in our present work we aim at measuring power density spectra of the type:

$$S_i(\omega) = K\omega^{-(1+b)}, \quad 0 < (1+b) \leq 2 \tag{2.12}$$

that have a smooth slope such as usually corresponds to very low frequency noise spectra. From the above considerations a good choice of the whitening function seems to be:

$$|H(\omega)|^2 = k_1\omega \tag{2.13}$$

in the frequency band of interest.

Introducing equations (2.12) and (2.13) into (2.7) we obtain:

$$S_o(\omega) = k_2 \, \omega^{-b} \tag{2.14}$$

where k_2 is a constant and $0 < |b| \leq 1$. Equation (2.14) represents a smooth power spectrum linearly related to the input power spectrum. Hence, the recolouring of the output data becomes a simple matter.

Now, by designing a filter with a voltage amplitude characteristic curve as $|H(\omega)| = k_3 \sqrt{\omega}$ in a wide band, we obtain a high-pass section behaviour in this band. Hence, the prewhitening and the high-pass section filter may be obtained by one and the same section in Fig.2.3. This high-pass section automatically filters out the very lowest frequencies, which may be regarded as slow drifts of the d.c. component and the input signal $\phi_i(t)$ is processed as having zero mean value.

31

Therefore, the procedure proposed with this type of prewhitening yields output values which are practically d.c. unbiased, increasing the accuracy of the power density spectrum analysis especially at low signal levels and at very low frequency values.

5. Required measuring time T and statistical error ε of a measurement

Assuming the sample record of $\phi_o(t)$ is averaged over a time interval T and corresponds to a stationary random process with zero mean value and with a smooth spectrum, for the time average of $\phi_o(t)^2$, in its frequency representation inside a bandwidth $\omega_o \pm B_e/2$, we have [2-6]:

$$\varepsilon^2 = \frac{\overline{(S_o(\omega_o) - \overline{S_o(\omega_o)})^2}}{\overline{S_o(\omega_o)}^2} \simeq (B_e T)^{-1} + \frac{1}{576}\left(\frac{B_e}{\ell(\omega)}\right)^4 \qquad (2.15)$$

where, ε = statistical error or normalised mean error of the estimate of $S_o(\omega_o)$

$S_o(\omega_o)$ = estimated value of the output power density at ω_o

$\overline{S_o(\omega_o)}$ = final estimate or average value of $S_o(\omega)$

$\ell(\omega)$ = is called the spectral bandwidth of the random process $\phi_o(t)$ and is given by: $\ell(\omega) = |S_o(\omega)/S_o''(\omega)|^{\frac{1}{2}}$

T = true averaging time in seconds

B_e = the bandwidth in Hz of the narrow-band resolution filter $H(\omega)$.

In the case where ε is relatively small, $\varepsilon \leq 0.2$, the sampling distribution of the mean value of $S_o(\omega_o)$ may be approximated by a normal distribution with mean value $S_o(\omega_o)$ and a standard deviation (s.d.) $\varepsilon.S_o(\omega_o)$. Then, in practice, for all repeated measurements the true value lies within the interval $S_o(\omega_o)/(1 \pm 2\varepsilon)$, with a 95 per cent. confidence level.

When the power spectrum is properly resolved the second term of equation (2.15), known as the bias error, will usually be negligible and (2.15) reduces to:

$\varepsilon = $ s.d. $S_o(\omega_o)$ / $S_o(\omega_o) \simeq (B_e T)^{-\frac{1}{2}}$ $\qquad (2.16)$

The resonant response of a linear system gives a properly resolved measurement if the physical bandwidth B_e of the analyser is $B_e < \frac{1}{4} B_{sr}$, where B_{sr} is the half-power point bandwidth of the narrowest peak in the power spectrum being measured. $B_e < \frac{1}{4} B_{sr}$ is taken as a practical criterion. This criterion should limit bias errors to less than 3%, when power spectra of physically random data are measured and $B_e T \gg 1$ is assumed [2-7].

An essential question still remains to be answered. What is the true bandwidth B to be introduced into equation (2.16)? For B we should take the noise bandwidth, i.e. the bandwidth of an assumed rectangular filter that passes through a white noise signal with the same mean square values as the physical filter. Then, when the input is white noise and we have a single-tuned filter with half-power bandwidth B_e, $B = \pi/2 \cdot B_e$. Thus in practice we have the relation:

$$\varepsilon \approx \left(\frac{\pi}{2} B_e T \right)^{-\frac{1}{2}} \tag{2.17}$$

Table I has been obtained using equation (2.17) for a bank of filters with equal Q factor of 5 and for the spot frequency values chosen in section 3 within the spectrum range 20 to 10^{-2} Hz.

Frequency: Hz	$\varepsilon = 7.5\%$				$\varepsilon = 5.0\%$				$\varepsilon = 2.0\%$			
	Days	hrs	min	sec	Days	hrs	min	sec	Days	hrs	min	sec
19.8				28.58			1	43			7	3.28
10.0				56.58			2	7.32			13	15.77
4.64			2	2			4	34.4			28	35
2.15			4	23			9	52.2		1	1	41.27
1.0			9	26			21	13.2		2	12	37.74
0.464			20	19.5			45	44		4	45	50.29
0.215			43	52		1	38	42		10	16	52.75
0.100		1	34	18.8		3	32	12.4		22	6	17.46
0.0464		3	23	15		7	37	20.5	1	23	38	23.17
0.0215		7	18	40		16	27	0.5	4	6	48	47.77
0.010		15	43	8	1	11	22	4	9	5	2	54.7
	Days	hrs	min	sec	Days	hrs	min	sec	Days	hrs	min	sec

If $\varepsilon = 7.5\%$ a total time of 1 day and 5 hours is needed to measure the spectrum of interest, while if $\varepsilon = 2\%$ the time needed rises to 17 days and 5 hours. Consequently, some compromise must be made between the desired statistical error and the frequency value under observation. High spot frequencies may be resolved with a 2% statistical error, while low frequencies with at most 5% error lead to a total measuring time of 3 days for the same spectrum range. A random measuring order will smooth out possible fluctuations of the estimates and the repetition of certain measurements will indicate if significant changes have taken place in the random process during the total measuring time of the spectrum.

6. The integrating-averaging power instrument

In the time domain the integrating-averaging power instrument of Fig. 2.1 may be regarded as being an autocorrelator (Fig. 2.4). In equation (2.11) the integration of the squared value of $\phi_o(t)$ is needed. In practice, $\phi_o(t)^2$ is given by $\phi_o(t) \cdot \phi_o(t+\tau)$ as τ tends to zero. By using an analogue multiplier, this product is easily obtained, since some phase shift or time delay exists in practice between the two inputs, although it should be as small as possible. The output of the multiplier is a voltage quantity of squared-volt units having very low frequency components, which when measured by any analogue reading instrument, will yield a fluctuating value and not a mean value as desired.
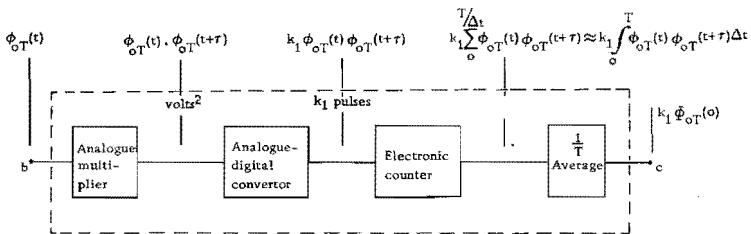

Fig. 2.4 Block diagram of the integrating-averaging power instrument.

Furthermore, as seen in section 5 the required measuring time T is at least 15 hours for the lowest frequency value. If an analogue integration, e.g. by a Miller integrator, is performed during the above time T, serious difficulties may be encountered with respect to drifts of the zero level and input currents as well as to the necessity of a large voltage condenser.

These difficulties can be avoided by using an analogue-to-digital convertor with a high sampling rate Δt, where $\phi_o(t)^2$ is continuously converted or sampled into a proportional numer of pulses. These can be added by an electronic counter yielding in practice a continuous integration over the time T. Averaging the integration over the observed time T, gives the autocorrelation function $\Phi_{oT}(\tau)$ for a delay time τ. For $\tau \to 0$ we obtain the average power of $\phi_{oT}(t)$.

The capacity of the counting operation is increased very considerably by the simple addition of a 6-digit mechanical counter which indicates the number of times the electronic counter saturates. With the instrument used, a 100-day integration can be reached at a counting rate of 100 K pulses a second before the mechanical counter also saturates.

Care must be taken that the sampling frequency $1/\Delta t$ is at least twice as high as the highest frequency present to avoid the introduction of aliasing. Half the sampling frequency is known as the folding or Nyquist frequency $f_N = 1/2\Delta t$. The term "aliasing" refers to the fact that high frequencies and low frequencies may share the same sampling points in time and thus an uncertainty is introduced with respect to the frequency value of the measurement being done. Hence, a safe way to reduce the possibility of aliasing is to filter out the high frequency components of $\phi_o(t)$ before it is sampled and to use a high sampling rate.

7. Sources of error

Under the term "sources" we wish to include the main causes that disturb the general trend of measurements, whether the source be a measuring procedure, a circuit type or a side effect in the realisation of an electronical approach.   **35**

In this section some practical compensations and corrections are pointed out. The main sources of error are listed below, although some have already been considered in the previous sections:

    a̲ Very low frequencies.

    b̲ Leakage of power through the spectral sidelobes and the tails of $H(\omega)$.

    c̲ Aliasing.

    d̲ The frequency selectivity procedure.

a̲ Very low frequencies

The true d.c. level of $f(t)$ can be easily set to zero by subtracting the mean value of the signal or, in practice, by introducing a large blocking capacitor in the circuit. But then, very low drifts of the mean value may still appear as ultra low frequencies, producing a large peak in the spectrum near to the zero frequency[2-8].

The best error compensation seems to lie in the application of a filter that prewhitens down to zero frequency. Indeed, use was made of such a prewhitening filter having a $k\sqrt{\omega}$ voltage amplitude characteristic curve and a d.c. blocking capacitor as its input.

Furthermore, throughout the measuring system, the use of differential amplifier stages with strong d.c. feedback will substantially contribute to low drifts. A large blocking capacitor may be placed at the input of the analogue-digital convertor to reduce the contribution of the d.c. offset level at the output of the analogue multiplier.

b̲ Leakage of power through the spectral sidelobes and tails of $H(\omega)$

This problem appeared in section 3. The practical solution is given by the combination of a low Q filter and a low-pass filter section. The cut-off frequency of the low-pass section is synchronised with the selective frequency value of the filter. The low-pass section decreases the contribution by leakage through the high frequency tail of the filter. The prewhitening filter attenuates the filter's tail contribution on the low frequency side.

<u>c</u> <u>Aliasing</u>

The problem of aliasing was considered in section 6. As a conse-
quence of the sampling introduced by the analogue-digital convert-
or, high frequency components appear as low frequencies.

The analogue-digital convertor used has a sampling rate of 10 μsec.
The corresponding Nyquist frequency is 50 kHz which is twice the
internal clock frequency of the analogue multiplier. Hence, the
sampling rate is sufficiently high to avoid aliasing.

The high frequency noise components do not alias because they are
attenuated by a by-pass capacitor to ground placed after the se-
lective filter and by the low-pass section of Fig. 2.3.

<u>d</u> <u>The frequency selectivity procedure</u>

The frequency selectivity with a bell-shaped characteristic curve
may be obtained by placing a Twin-T circuit in the feedback loop
of an operational amplifier. The circuit diagram is shown in Fig.
2.5, where A is a differential-stage amplifier. Owing to the se-
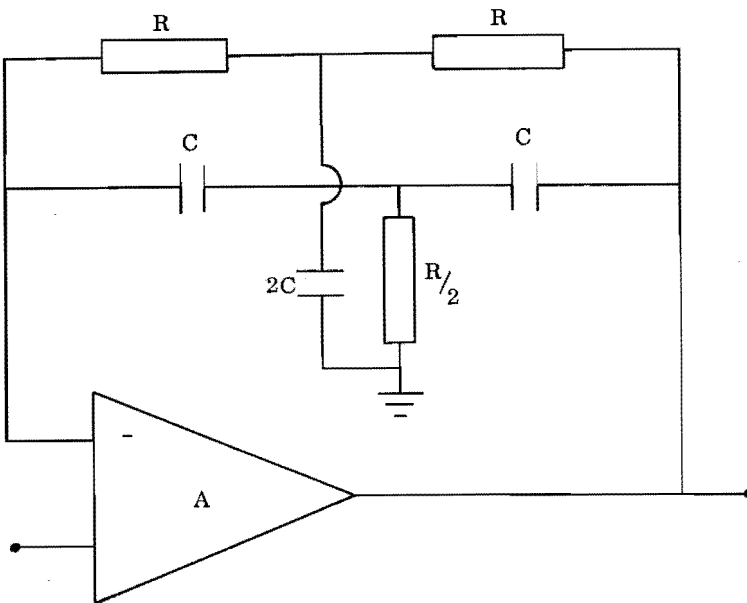
Fig. 2.5 Selective amplifier with a Twin-T fed back circuit.   **37**

lectivity at very low frequencies, down to 10^{-2} Hz, it is conven-
ient to have a d.c. path in the feedback loop. The selectivity is
obtained by varying simultaneously the values of the three capaci-
tors or of the three resistors.

Now, shot-noise power is proportional to the d.c. current and
flicker-noise power to the square of the d.c. current. Thus, with-
in the spectrum band of interest (10^{-2} Hz to 20 Hz), if the three
resistors of the Twin-T circuit are the variable elements, they
will be changed by a factor of 2.10^3 and consequently also the d.c.
current. Therefore, this selectivity procedure will yield a con-
siderable change in the flicker and shot noise power of the Twin-T
circuit.

On the contrary, with variable capacitors, the d.c. current in the
Twin-T circuit will be constant and the same noise producing ele-
ments will remain in the circuit for all frequency values of meas-
urement.

Bull[2-9] came across a similar situation in a selective amplifier,
but he said he did not know whether the excessive noise in his case
arose in the valves known to have low-noise levels or in the cir-
cuit resistors or again, perhaps from the method of reducing the
bandwidth. It seems probable that the cause was the selectivity
procedure realised by changing the resistor values.

From the above considerations the correct selectivity procedure to
be applied to low-noise operation at very low frequencies appears
to be realised by varying simultaneously the three capacitors and
not the resistors.

THE MEASURING CHANNEL

Summarising the block diagrams of Figs. 2.1, 2.3 and 2.4 of chap-
ter II with the practical considerations already mentioned, we ar-
rive at a convenient lay-out for a low-frequency noise power meas-
uring channel.

Now, assuming that the pre-amplifier and the amplifiers have a flat
band response down to d.c. and a broader bandwidth than the spec-
trum band in question, the measuring system proposed in chapter II
is not affected either in the time domain or in the frequency do-
main. Therefore, we will design and construct the following meas-
uring channel as shown in Fig. 3.1.
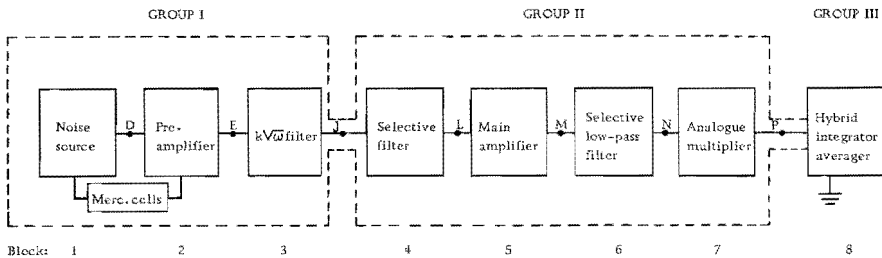
Fig. 3.1   The measuring channel

Three block-groups can be distinguished in Fig. 3.1. The first
group, which encloses blocks 1, 2 and 3, delivers at point J a suf-
ficiently strong voltage noise signal $\phi(t)$ with a white noise power
spectrum for a 1/f input noise spectrum within the frequency range
of interest, viz. 10^{-2} Hz to 20 Hz. The second group elaborates the
selective frequency window centered at ω_o and delivers at point P a
proportional squared value of the voltage noise. Group III does the
integration and averaging of $k\phi^2(t)$ over the prescribed observation
time T.   **39**

The blocks of group I are thermally, electrostatically and magnet-
ically shielded to avoid as much as possible any external interfer-
ence, especially from the frequency of the power mains. The first
group is energised by mercury cells and has its shield materially
joined to that of group II by means of a sleeve shield, inside
which a coaxial cable transmits the signal from group I.

Group II is also thermally and magnetically shielded. It is powered
from a floating output power supply; the same applies to all its
blocks. Their common ground is earthed at the grounding point of
the integrating block, the unique earth point for the whole meas-
uring channel. The output signal at point P is transmitted with a
coaxial cable within a sleeve shield, grounded at its end.

Inside groups I en II silica gel is enclosed to maintain a dry sur-
rounding. In the following pages we will consider each block dia-
gram of the lay-out of Fig. 3.1.

1. Block I: Noise sources

Two types of noise sources have been measured, namely carbon-film
resistors and bipolar transistors of the npn and pnp types. The
noise sources are operated at very low current levels, viz. 1 to 2
μA.   It was suspected that such an operating mode would allow the
appearance of relevant features obscured at higher current levels
by, for instance, dissipation effects.

The different noise-source networks are shown in Fig. 3.2. A noise
voltage is evolved by the noise source between points F and G, and
is fed by a large dry tantalum capacitor, C_1, into the pre-amplifi-
er; the first stage of which is also shown in Fig. 3.2a. The pre-
amplifier has a differential input stage with equal source resis-
tors (50 kΩ) connected as in a bridge type network and d.c. bal-
anced at the two bases. After the adjustment of the potentiometer
50 kΩ (or 2 kΩ) in Fig. 3.2-a (or b and c), point F has the same
d.c. level as point D. The same is done in the pre-amplifier for
points F' and D'. Therefore, by means of this adjustment the leak-
age currents of capacitors C_1 and C_2 are very small, of the order
40 of less than 10^{-10} A, and the coupling of the noise source to the
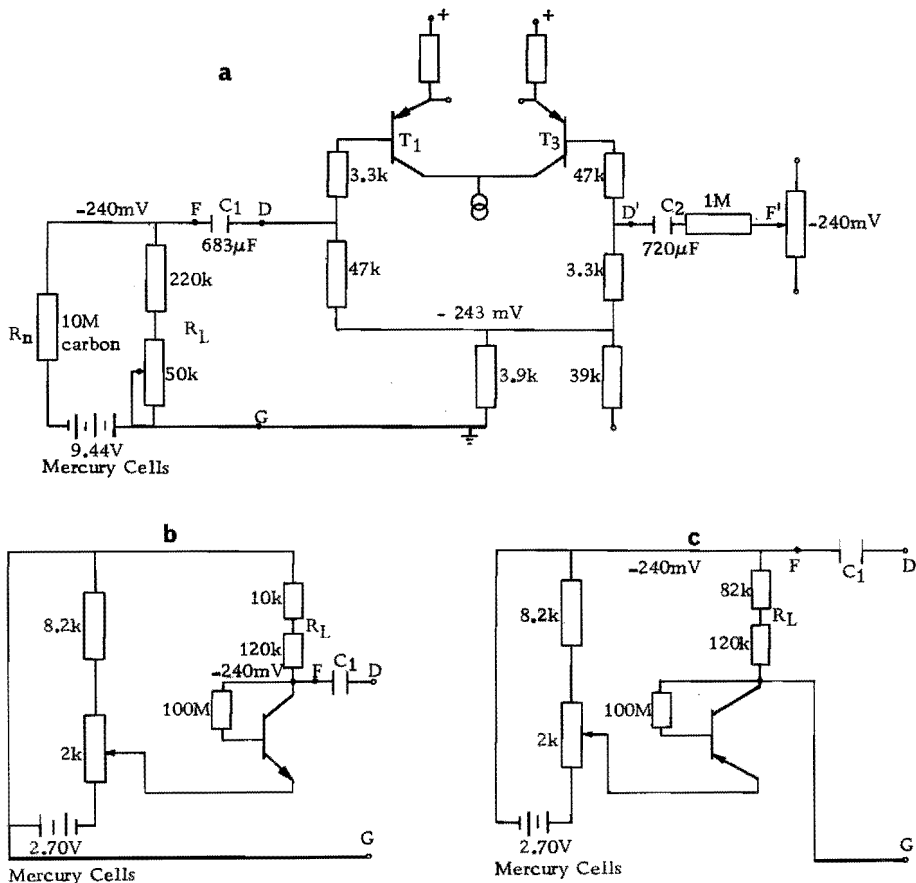
*Fig. 3.2 Noise sources. a) carbon resistor, b) npn transistor,
c) pnp transistor.*

pre-amplifier does not unbalance substantially the d.c. level of
points D and D'. The pre-amplifier always operates in the same con-
ditions whether a noise source is connected or not.

Apart from the noise source itself all resistors are of the metal
film type, with a temperature coefficient of ± 25 ppm/°C and a
specified noise voltage figure of 0.1 μV/V. The potentiometers are
wirewound and hence practically free from flicker noise. With re-
spect to the noise contribution of C_1 and C_2 we may mention that
capacitors are the least noisy electronic components and we believe
that their noise contribution may be neglected completely in this
network operation.

The energy of the circuit is supplied from mercury cells which are known for their very stable output voltage at low drain currents, for their relatively high current capacity (3400 mA.h for the type used), and for their very low voltage noise of approximately 4 μV_{pp}/cell, max.

As noise-resistor source we used cracked-carbon film resistors. They are known to be made of small-size crystal graphite and larger amorphous coal grains, and possibly with oxygen atoms as bridges between the graphite and the coal. The resistors had a standard value of 10 MΩ ± 10%, 1/16 W, and when measured in the bandwidth 0.06 Hz to 60 Hz, noise peak voltages from 40 μV to 400 μV were observed for the different units under consideration.

For the case of a transistor noise source a 100 MΩ resistor was introduced for biasing the transistor. The resistor was made of an inorganic film deposited on a ceramic rod and was hermetically glass-sealed against moisture and other contaminants. Its temperature coefficient was 0.5%/$^\circ$C and its low output noise is negligible on the load resistor R_L.

Noisy transistors were chosen as sources owing to their observed burst noise with an approximate repetition rate of 0.1 sec or longer, and thus the burst noise is observable in the frequency range of interest. The burst voltages at point F were from 100 μV to 400 μV for the different transistors, when operated at a collector current of 1.5 μA.

2. Block 2: Pre-amplifier

Sometimes, in order to obtain a very low drift amplifier, quite a number of compensating elements are introduced in the circuit. The final result may be an increased output noise level. Therefore, our aim is to design a pre-amplifier as simple as possible with the smallest number of active and passive elements. At the same time a transistor operating mode is to be found that can combine the advantages of low-drift and low-noise operation.

42 The "Hushed-mode" operation was first suggested by Volkers and

Pederson[3-1]. The hushing operation of a transistor consists in bi-
asing the transistor with practically zero voltage drop from col-
lector to base. The authors pointed out that an appreciable improve-
ment is obtained in the current noise behaviour and on the 1/f noise
spectrum of a transistor operated in the hushed-mode. This improve-
ment will always be obtained even if the transistor shows low noise
figures for its normal mode operation. Therefore, hushing a tran-
sistor will yield a reduced noise behaviour in much the same way as
negative feedback is the tool for obtaining ultimate amplifier line-
arity, independant of the non-linear characteristics of the active
element.

A closer look at the hushed-mode brings forward some properties of
this low noise operation which are also features used for low drift
in low-level signal amplification and for low distortion operation.
These features are summarised as follows:

(a) low collector current operation[3-2]
(b) low collector junction temperature[3-3, 3-4, 3-5]
(c) improvement of the common-mode rejection for a differential
    stage[3-6]
(d) practically constant current gain
(e) reduction of the non-linearities in transistors[3-7]
(f) possibility of using a complementary transistor-compound stage[3-8]

Let us now first consider a transistor stage under the following
points of view: (A) Low drift, (B) Low noise, (C) Low distortion.
These points of view will include the above features in a non-sys-
tematic manner. Then, secondly, we will realise an actual pre-ampli-
fier according to these points of view.

(A) Low drift

Transistor temperature problems are not necessarily difficult. But
the design of a high-performance amplifier requires great attention
to many details and some amount of skill if the transistor parame-
ters are to be sufficiently stable over a long period of time.

In an amplifier the main source of drift is to be found in the first
stage and to a much smaller extent in the second stage, caused by   **43**

In silicon transistors at low collector-to-base voltages ΔI_{CBO} is very small, viz. of the order of 10^{-12} A/^{o}C, which makes the fourth term of (3.6) negligible. The third term is reduced considerably by the hushed-mode operation, as will be seen in (3) I_{CBO}. For equal source resistance $R_{s_1} = R_{s_2} = R_s$, the second term $(\Delta V_{BE_1} - \Delta V_{BE_2})/R_s$ becomes negligible as follows from the considerations about equation (3.3). Therefore, the main contribution is the first term and we arrive at:

$$\Delta I_{B_1} - \Delta I_{B_2} \simeq I_{B_1} \frac{\Delta \beta_1}{\beta_1} - I_{B_2} \frac{\Delta \beta_2}{\beta_2} \tag{3.7}$$

According to (3.7) the input drift is small because $\Delta\beta/\beta$ is typically less than $1\%/^{o}$C. We can make it still lower by decreasing the operating current I_c and by using a high β. Therefore, a second conclusion is that the input transistors should be a matched pair in β values at equal V_{BE} voltages; high β values at very low I_C are desired.

Fortunately, large β values are possible in planar transistors even at practically zero V_{CB} and at very low operating currents. We have found experimentally that at an I_C of 10 µA and at V_{BE} constant, in some transistor types the value of β at V_{CB} equal to 100 mV is decreased only by 10% with respect to its value for V_{CB} equal to 2 V. The cause of the small decrease in β seems to be the high collector-to-base contact potential, which is 0.7 V for silicon. In germanium transistors this contact potential is only 0.30 V and the β values are decreased by a factor 2 to 3 for operating conditions similar to the above. Thus, silicon transistors should be used for the hushed-mode operation.

(3) I_{CBO}

The leakage current I_{CBO} consists of four components. Two of them, a and b, are mainly due to temperature action and the other two, c and d, to the voltage.
a. In the base region, for any temperature pairs of electrons and holes are generated.

<u>b</u>. Under the influence of thermal action, too, extra electrons and holes are generated on the collector surface by surface energy states.

<u>c</u>. A third component arises in the collector depletion region, the volume of which depends on the material resistivity, the junction area and the voltage V_{CB} across it.

<u>d</u>. Surface impurities, moisture and other insulating materials as SiO_2 constribute to the fourth component, which depends also on the surface potential.

Now, operating the transistor at low current and voltage bias means lowering the operating temperature of the transistor and, therefore, decreasing components <u>a</u> and <u>b</u>. At the same time the hushing operation will decrease component <u>c</u> and reduce the excess current due to an inversion layer[3-16, 3-17] in the base region produced by the surface potential.

Since in silicon transistors I_{CBO} doubles for every $15°C$ increase in temperature[3-18], it is important that I_{CBO} is small in order to neglect the third and fourth terms in equation (3.6). We may conclude that the hushed-mode operation is appropiate for low drifts.

(4) Improved collector-source current

In d.c. coupled amplifiers intrinsically stable current sources are important, since fewer compensating elements are needed and thus the total noise level is reduced indirectly.

Baxandall and Swallow[3-19] have designed a new current source circuit. Fig. 3.3 is a slightly modified version to be used as a one-half circuit of a differential stage. Essentially, it is a pnp-npn compound transistor which may be considered as a pnp unit between the points E, B, C. It has a very high input impedance and a high d.c. current amplification factor. The input transistor is hushed-mode operated.

(i) <u>Temperature compensation</u>. The main features of its temperature analysis are as follows.

(i-1) The voltage change ΔV_{BE} from points B to E due to the effects **47**
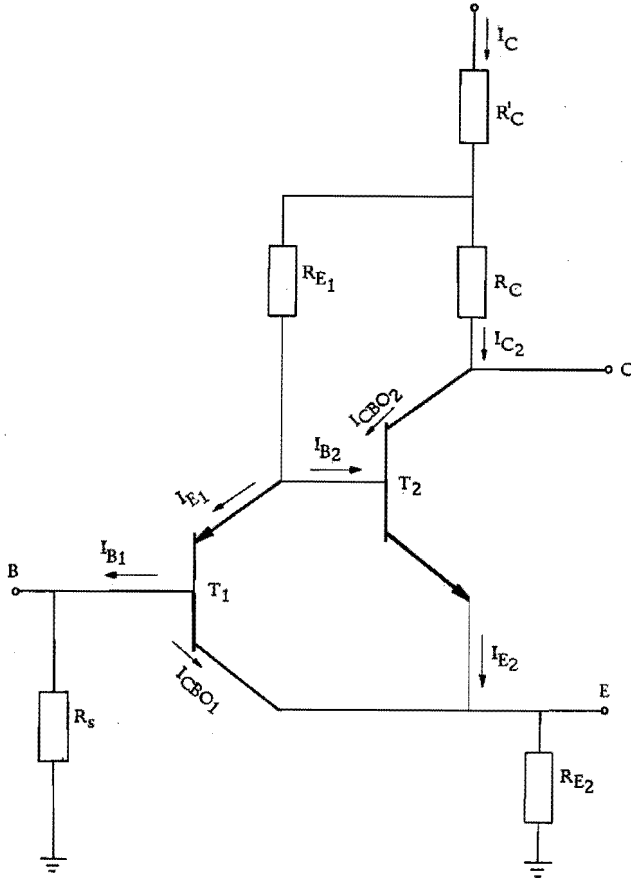
Fig. 3.3   The compound transistor stage

of ambient temperature changes on the emitter-base voltages of the
two transistors will largely balance against each other. This ΔV_{BE}
across the current determining resistor R_{E_2} produces an output cur-
rent variation, ΔI_{C_2}, at point C. Assuming ΔV_{BE} to have a negative
temperature coefficient of 0.25 mV/°C, then for 2.5 V across R_{E_2},
$\Delta I_{C_2}/I_{C_2} = (-0.25 \text{ mV}/2.5 \text{ V})/°C = -0.01\%/°C$.

But ΔV_{BE_1} produces a change in I_{E_1} across R_{E_1} and hence another
change in I_{C_2}, $\Delta I_{C_2}'$. Assuming 1V across R_{E_1} and across R_C', with I_{E_1}
being 10% of I_{E_2} and ΔV_{BE_1} equal to -2.8 mV/°C, the output current
change is $\Delta I_C/I_C = - (2.8 \text{ mV}/(1V + 1V \cdot 10))/°C = -0.025\%/°C$. Thus
at the output point C a total change of I_{C_2} smaller than 0.04%/°C
may be expected.

48

(i-2) Since the total I_{CBO_2} is transmitted to the emitter of T_2 via T_1, ΔI_{C_2} caused by ΔI_{CBO_2} is almost compensated by the negative feedback action of R_{E_2}. The transistor T_1 is hushed-mode operated and therefore the I_{CBO_1} is negligible.

(i-3) The variation of the current gain, $\Delta\beta_2$, causes I_{B_2} to change, but this change is also transmitted to the emitter of T_2 and almost compensated.

(i-4) The compound transistor CBE has no compensation for $\Delta\beta_1$ caused by temperature variations. Since I_{E_1} is taken as 10% of I_{E_2}, we should expect $\Delta\beta_1 \ll \Delta\beta_2$.

(i-5) The temperature variations of I_{B_1} due to ΔI_{BCO_1} will be very small since T_1 is hushed-mode operated. Thus the input thermal drift of the silicon compound transistor is small even for large R_s base resistances.

(ii) Current amplification

The d.c. current amplification factor of the compound transistor, β_{cp}, defined as I_{C_2}/I_{B_1} is:

$$\beta_{cp} = \beta_2 I_{B_2}/I_{B_1} = I_{E_2}/I_{E_1} \times (\beta_1 + 1) \cdot \beta_2/(\beta_2 + 1) \qquad (3.8)$$

Assuming $\beta_2 \geq 100$ in T_2:

$$\beta_{cp} = (\beta_1 + 1) \cdot I_{E_2}/I_{E_1} \qquad (3.9)$$

Therefore, if we assume I_{E_1} to be 10% of I_{E_2} and β_1 equal to 100, $\beta_{cp} = 10^3$.

(iii) Input impedance.

For a C.E. stage and taking the small signal current amplification factor to be equal to β, the input impedance is given by $(\beta+1)(r_e + (1-\alpha) r_b)$, where r_e and r_b are the total resistance on the emitter and base. Considering Fig. 3.3 to be one half of a differential stage, point E is virtually grounded and the input impedance becomes:

$$Z_{in} = (\beta_1 + 1)\left[r_{b_1}(1-\alpha_1) + r_{e_1} + R_{E_1} // (\beta_2 + 1)(r_{b2}(1-\alpha_2) + r_{e_2}) \right] \qquad (3.10)$$

49

where // means "in parallel". Neglecting the contributions due to
the factor $(1-\alpha)$ and replacing the dynamic emitter resistance by
its equivalent $26/I_E$ Ω (I_E in milliamperes), we arrive at:

$$Z_{in} = (\beta_1+1)\left[\frac{26}{I_{E_1}} + R_{E_1}//(\beta_2+1)\frac{26}{I_{E_2}}\right] \tag{3.11}$$

(B)-Low-noise design

It is known that the noise of a transistor with conventional oper-
ating parameter values increases when the collector current is de-
creased below a certain optimum value. But it was found[3-1] that e-
ven when the noise of a transistor in a conventional circuit is low,
it can always be reduced by the hushing principle. Thus, there is an
optimum operating current with a hushed-mode collector-to-base volt-
age.

Now, just from the point of view of low noise figure, an optimum op-
erating current I_E may be obtained. Noise factor is defined as the
ratio of the total mean square noise voltage at the output of a
transistor to the mean square noise voltage at the output resulting
from the thermal noise in the source resistance R_s. The noise fac-
tor of a transistor in a C.E. configuration is given by[3-20]:

$$F_E = 1+r_b/R_s+r_e/2R_s+1/\beta.1/2R_s r_e\left(1+f/f_c.\sqrt{\beta/\alpha}\right)\left(R_s+r_b+r_e\right)^2 \tag{3.12}$$

where r_b is the incremental base resistance, r_e the incremental e-
mitter resistance, f_c the cut-off frequency.

The second term of equation (3.12) is the noise in r_b, the third
term represents the noise due to r_e and the fourth term is the noise
in the collector. Replacing r_e by its equivalent function of I_E as
above, and assuming β practically independent of I_E, for $f << f_c$,
equation (3.12) becomes:

$$F_E = 1+r_b/R_s+26/2I_E R_s+I_E\left[R_s+r_b+26/I_E\right]^2\Big/52\beta R_s \tag{3.13}$$

50 Differentiating with respect to I_E and equating to zero, we obtain

the optimum operating current $I_{E_{opt}}$ expressed in milliamperes for the minimum noise figure, which is given by:

$$I_{E_{opt}} = 26\sqrt{\beta + 1}\big/(r_b + R_s) \tag{3.14}$$

Re-introducing r_e into (3.14) we arrive at the optimum R_s for minimum noise figure:

$$R_{s_{opt}} = r_e\sqrt{\beta + 1} - r_b \tag{3.15}$$

We note that the minimum noise figure is obtained for a source resistance value lower than when impedance matching conditions are met at the input; here, Z_{in} is for a CE configuration and is given by $r_b + r_e(\beta + 1)$. Hence, this mismatching situation means a loss of power transfer from the source to the transistor, although it yields a better signal-to-noise ratio. For a mismatching situation with R_s/Z_{in} equal to 10^{-1} it is possible to obtain a noise figure of 1 dB with a relative power loss of approximately 5 dB only[3-21], [3-22].

Owing to the active element, the input stage always gives some power amplification. Therefore, when operating for low noise conditions, the value of R_s should be actually chosen more from the point of view of low thermal drift and noise figure than from impedance matching considerations.

The last term in equation (3.12) represents the noise in the collector, but the influence of the surface collector leakage current I_{CL} as well as the collector reverse saturation current I_{CS} has been neglected. Now, Hurley[3-23] has considered in detail the noise sources within a transistor. The mean square collector semi-conductor noise voltage, $\overline{(e_c^2)}$, is assumed to be:

$$\overline{(e_c^2)} = K_c\left(V_{CB}/R_{CL}\right)^2 r_c^2 \, \Delta f/f \tag{3.16}$$

where K_c is a constant proportional to the volume of the material, R_{CL} is V_{CB}/I_{CL}. In practice I_{CL} is the main component of I_{CBO} and   **51**

much larger than I_{CS}. From (3.16) we see that the hushed-mode operation will almost eliminate this noise source and then equation (3.12) will represent a noise-figure behaviour closer to reality, with the main source of noise appearing in the emitter.

Therefore, from equations (3.12), (3.15), and (3.16) we conclude that the transistor should be operated in a hushed-mode, at a very low optimum current level and with an approximate impedance mismatching ratio between 10^{-1} to 10^{-2} in order to obtain a very low noise figure of 1 dB.

(C) Low-distortion considerations

Let us now give some consideration to the linearity of a transistor operating at low currents and bias voltage. Some authors have analysed the cross-modulation and the intermodulation noise in transistors[3-21, 3-24, 3-25]. Here we will consider the input and output diodes of a CE configuration with respect to their linear behaviour.

Let the output current of the signal i_c be expressed as a function of the operating voltage, v_c, i.e. $i_c = f(v_c)$. Then, expanding i_c into a Taylor's series around an operating point v_{c_1}, the signal current is expressed as a function of its linearity and non-linearities:

$$i_c = i_c\bigg|_{v_{c_1}} + \frac{1}{1!}(v_c - v_{c_1})\frac{di_c}{dv_c}\bigg|_{v_{c_1}} + \frac{1}{2!}(v_c - v_{c_1})^2\frac{d^2 i_c}{dv_c^2}\bigg|_{v_{c_1}} +$$

$$+ \frac{1}{3!}(v_c - v_{c_1})^3\frac{d^3 i_c}{dv_c^3}\bigg|_{v_{c_1}} + \ldots \quad (3.17)$$

It is known that the intermodulation distortion is caused by a non-linearity or curvature of second and higher even orders, while a curvature of third or higher odd orders produces cross-modulation[3-21, 3-24, 3-25]. For our present analysis and measurements we are interested in reducing the intermodulation distortion.

52 Now, a point of inflexion of a curve corresponds to a contact of

second order$^{3-26}$. Therefore, operating the output diode of the tran-
sistor at the inflexion point of the static characteristic curve
will yield a vanishing second derivative at v_{c_1} in the Taylor's se-
ries expansion of i_c, and consequently the intermodulation distor-
tion is cancelled. The static characteristic curve of the collector-
base diode is shown in Fig. 3.4-a. As the operating base current I_B
decreases, the curves become more parallel to the voltage axis and
the inflexion points P are shifted to lower V_{CE} values and conse-
quently to lower V_{CB} values. It is seen that for very low operating
currents, if the inflexion point is chosen as the operating point,
the transistor becomes operated in a hushed-mode and will produce
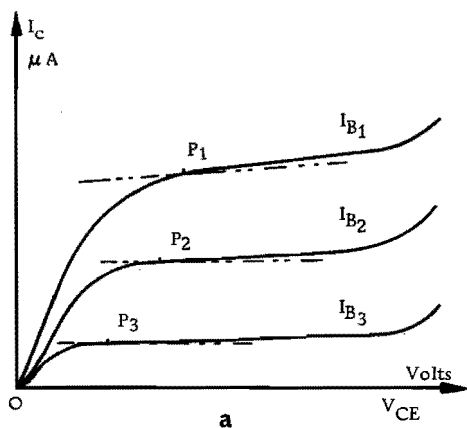low distortion.

*Fig. 3.4 Static characteristic
curves of a C.E. configuration; si-
licon junctions. a) output curve,
b) input diode, semilog scale,
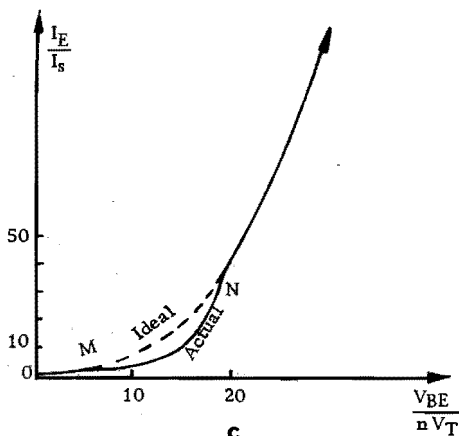c) input diode, linear scale.*

53
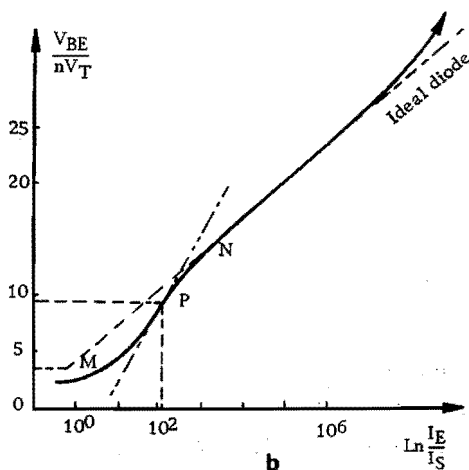
Fig. 3.4-b is taken form Moll[3-27] and represents the static characteristic curve of the ideal input emitter-base diode given by the relation $I_E = I_s \cdot (\exp qV_{BE}/nkT-1)$, dotted line. Here, kT/q is the thermal potential V_T, which is approximate 26mV at room temperature. I_s is the saturation current of the reverse-biased diode and n is a parameter, $1 \leq n \leq 2$. Having neglected the term $-I_s$ in the above expression, it is represented on a semilog scale in Fig. 3.4-b. But in practice the diode follows the "actual" curve. At low current values we note an increase of the slope[3-28].

When Fig. 3.4-b is represented on a linear scale we obtain Fig. 3.4-c and we note that the MN section of the actual diode curve has an increased slope with respect to the ideal curve. Therefore, the curve becomes more linear than for the ideal diode expression with the possibility of having also an inflexion point at a very low emitter current value. Hence, at very low I_E values the linearity of the input diode is improved and, in a transistor, corresponds to the situation of being hushed-mode operated.

Therefore, from the considerations made throughout parts (A), (B), and (C) we conclude that the hushed-mode operation in transistors leads to low drift, low noise and low distortion operation.

(D) Pre-amplifier circuit

The circuit of the pre-amplifier, Fig. 3.5, consists of three differential stages. The first two stages are designed upon the current source of Fig. 3.3 with R_{E_2} replaced by a better current source, namely a transistor, T_5, T_{10}. Each of the differential stages is made up of an emitter follower and an amplifier section. The signal is fed back from the output of the second stage via T_{12} to the second input of the first stage, T_3. The third stage constitutes a simple differential amplifier, $T_{11} - T_{13}$.

High input impedance is obtained by using the temperature compensated compound transistor. The use of current sources as of Fig. 3.3 in a differential arrangement leads to a second order temperature compensated stage, as implied by the circuit configuration. The contribution to the output drift of possible temperature variations still

54
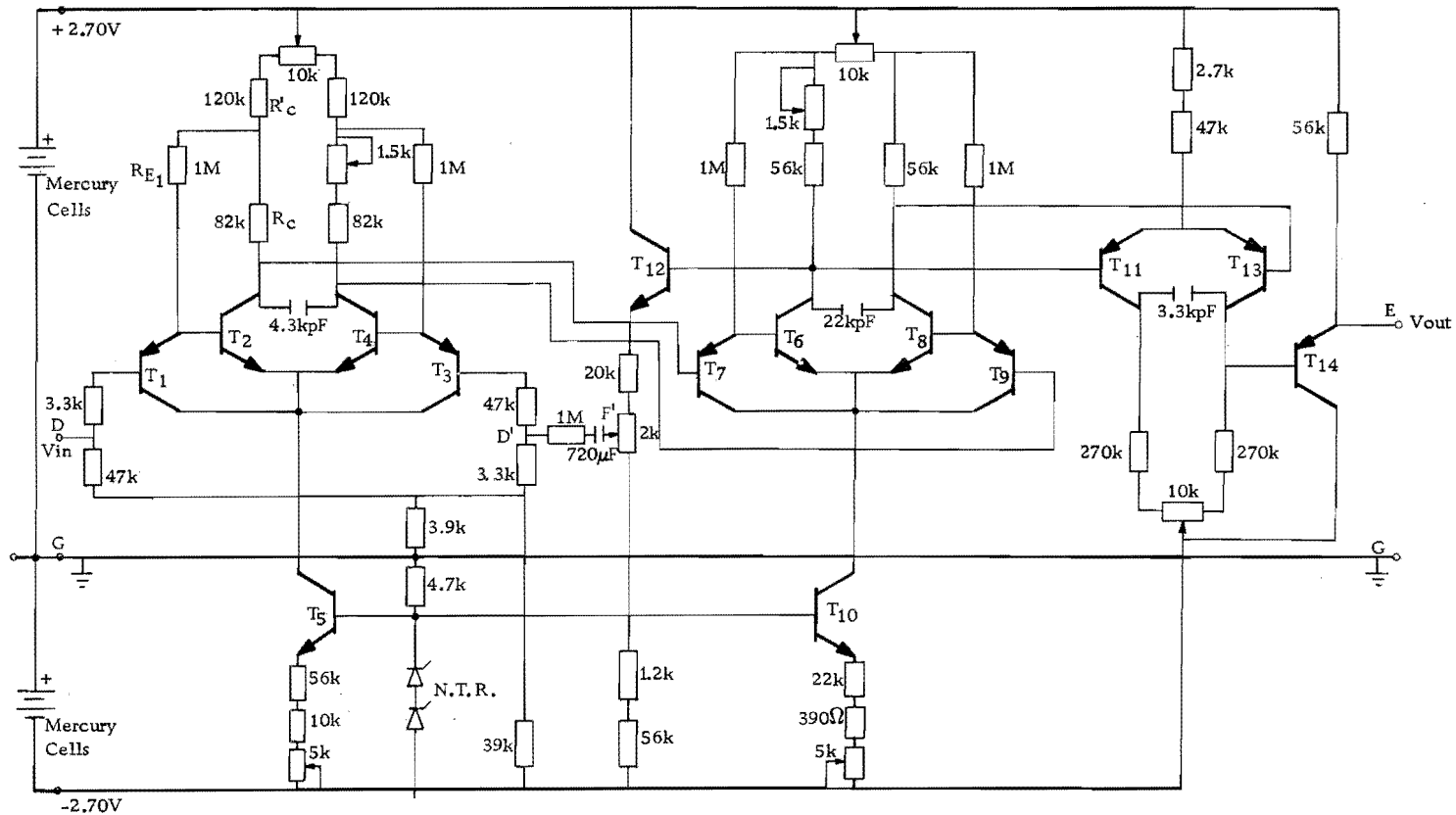
Fig. 3.5   Low noise and low drift pre-amplifier circuit

present are decreased by two effects. First, the transistor pairs T_2-T_4 and T_1-T_3 have matched β values within 2% for the same V_{BE} bias conditions. Secondly, the transistors of each pair are located on the same crystal chip and the pairs are placed one next to the other. Thus, the temperature and parameter variations of one half, T_1-T_2, of the differential stage are equal to those of the other half, T_3-T_4. The current source T_5 of the stage is also on the same crystal chip as T_2-T_4, (BFX-16), and temperature-compensated on the base by two negative temperature resistors (N.T.R.) of a barrier type. All these considerations can also be applied to the second stage.

The constant bias voltage of the input differential stage is obtained by the potential divider of 39 kΩ and 3.9 kΩ. The input circuit resistors are matched within 10^{-4} in order to have practically identical base resistances, with a resistance temperature coefficient of 25 ppm/$^\circ$C. The other resistors in Fig. 3.5 are also of thin metal film and have also very low noise.

By operating points D' and F', as well as D and F (see section 1), at the same d.c. level, the leakage currents of the tantalum capacitors placed at points F' and F do not affect the input base currents of approximately 10 nA.

All the transistors are operated at very low currents, namely, T_1 at 1 μA, T_2 at 10 μA. In the second stage, T_7 has an emitter operating current of 1.7 μA and T_6 of 22 μA. The same may be said of the other half section of these stage respectively. In the third stage, T_{11} and T_{13} have a d.c. current of 7 μA and the d.c. output level is practically at zero volts.

By adjusting the 10 kΩ potentiometer in the first stage, it is possible to obtain indentical V_{BE} for T_2-T_4. Then by adjusting the potentiometer 1.5 kΩ, both collector voltages are made identical and the second stage has a balanced d.c. input base voltage. This adjusting method is repeated in the second stage yielding the balanced

56 input base voltages of the third.

The first two stages are operated in a hushed-mode, with a V_{CB} of 50 mV for the emitter follower section and of 300 mV for the amplifier section. Therefore, the properties of low thermal drift, low noise and low distortion may be expected from this pre-amplifier circuit.

A capacitor placed between the collectors of each stage limits the bandwidth, yielding a -3 dB point at 60 Hz in the frequency response of the pre-amplifier.

The over-all voltage gain can be obtained by calculating the voltage gains of each stage and considering the feedback action from the second stage to the first. But owing to the complexity of each differential stage with its own feedback path, even an approximated calculation becomes troublesome and some of the transistor parameter values need to be known at the actual operating currents. Anyhow, the experimentally observed value was approximately 5.10^3.

The input impedance, according to (3.11), with a β_1 value of 100, is 50 MΩ. The long term thermal drift was observed to be 0.5 $\mu V/^oC$ at the input, while the input noise voltage in the 0.06 - 60 Hz frequency band was of the order of 10^{-7} V, peak to peak. This agrees with the later observation on the noise of the total channel, which is mainly due to the noise of the pre-amplifier. The channel turned out to have an input equivalent noise resistance R_n of 25 kΩ at room temperature. Its spectrum is white down to 3Hz and then it increases as $\omega^{-\beta}$, where $\beta = 1.68$ (see Fig. 4.1).

The pre-amplifier is energised with $\pm$ 2.7 V from mercury cells. A total amount of 300 μA operating current is needed and the power consumption is 1.5 mW.

3. Block 3: Wide-band prewhitening filter

The considerations in chapter 2, section 4, make us interested in a prewhitening filter with a transfer function $|H(\omega)|$ proportional to $\sqrt{\omega}$. Then for any frequency component ω of the signal, the output v_o and input v_{in} amplitudes of the voltage are related by:

$$v_o = k \sqrt{\omega} \, v_{in} \qquad\qquad (3.18)$$

Zaalberg van Zelst[3-29] has designed a filter that follows equation (3.18) within a certain frequency range. Such a filter is shown in Fig. 3.6. The appropriate values of resistors and capacitors for the frequency range 10^{-3} to 50 Hz are given below. The component pair C_o-R_o constitutes a high-pass section filter with a slope of 6 dB/octave. The seven series branches R-C placed in parallel with R_o reduce the slope to 3 dB/octave. Since there is a capacitor at its input the d.c. component and the ultra-low frequencies of the input signal are blocked.
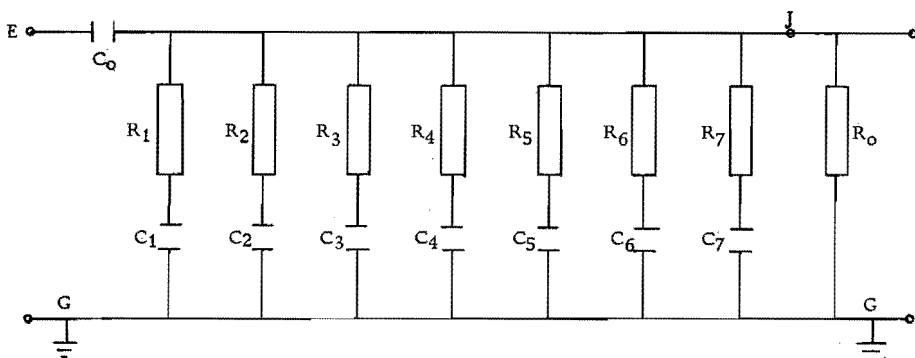
Fig. 3.6. Wide-band prewhitening filter, $k \sqrt{f}$

The actual values have been realised within 10^{-4} of the prescribed values. The capacitors used are made of polysterene which is the dielectric with characteristics closest to those of mica. The resistors are of the metal film type for values up to 1.5 MΩ; three high-quality low-noise carbon resistors APKD are used for larger values. The R_o resistor is actually the input impedance of the following block 4. The R-C values are given below:

C_o : 63.792 kpF R_o : 6.5000 MΩ

C_1 : 3.3000 µF R_1 : 7.1890 MΩ

C_2 : 1.5412 µF R_2 : 3.8233 MΩ

C_3 : 0.79868 µF R_3 : 1.9526 MΩ

C_4 : 0.41293 µF R_4 : 1.0042 MΩ

C_5 : 0.21236 µF R_5 : 519.09 kΩ

C_6 : 108.44 kpF R_6 : 268.97 kΩ

C_7 : 57.656 kpF R_7 : 125.64 kΩ
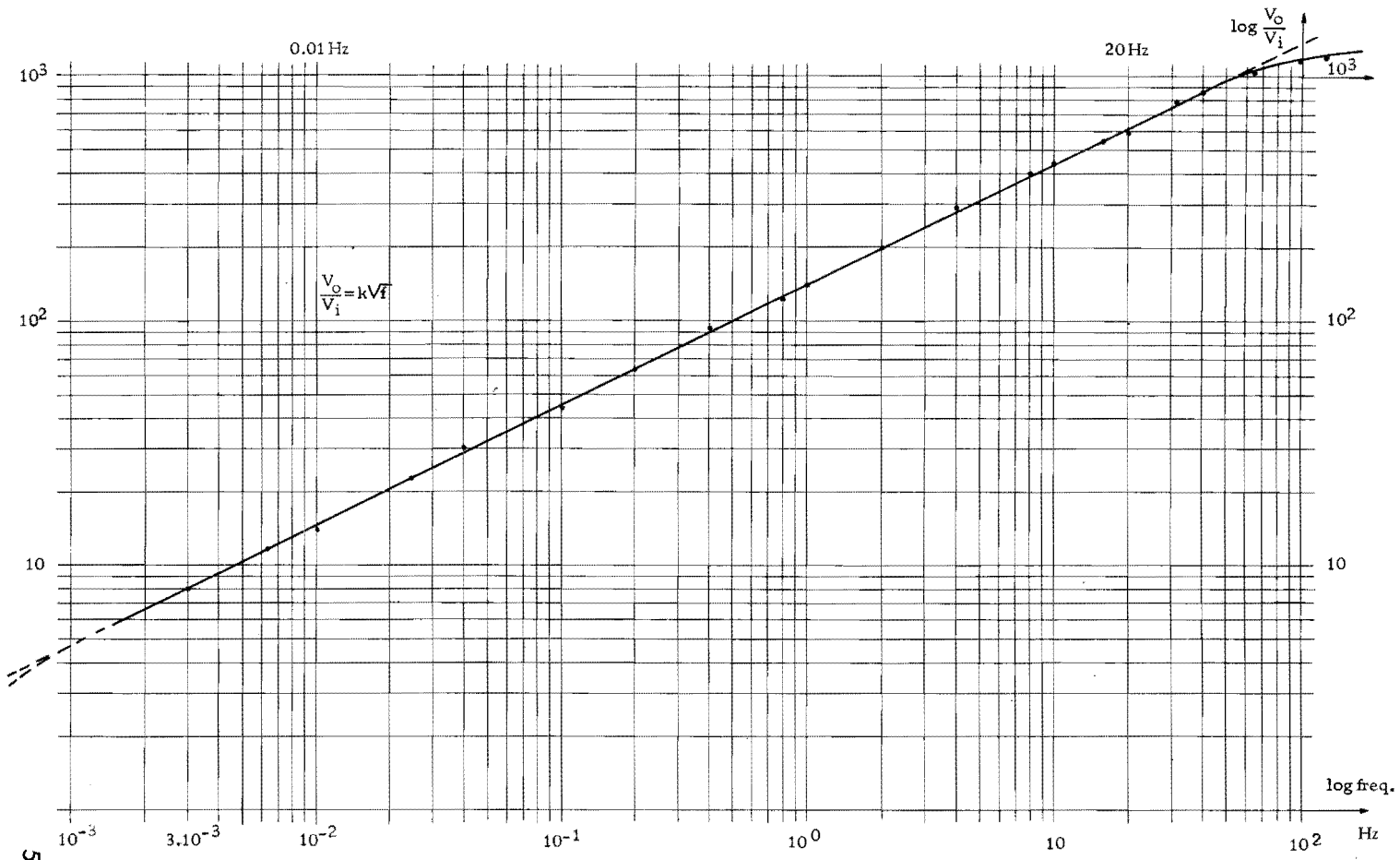
Fig. 3.7 Amplitude transfer characteristic curve of the filter $k \sqrt{f}$

$$\frac{V_o}{V_i} = k\sqrt{f}$$

The measured response of the filter of Fig.3.6 is shown in the graph of Fig.3.7 on a log-log scale. The ratio v_o/v_{in} follows a $k\sqrt{\omega}$ law within ± 2.0% in the frequency range 10^{-2} to 20 Hz, yielding a power spectrum $|H(\omega)|^2$ which follows a $k^2\omega$ law within less than 4% in the above frequency range.

4. Block 4: Ultra-low frequency active filter

When designing active filters the use of an operational amplifier with a selective network is a straightforward procedure. For frequencies below 10 Hz, L-C selective networks are not convenient since large values of C or L are needed, which are bulky in size and sensitive to external influences, especially the coils. Capacitors, however, are by far less sensitive to pick-ups at low frequencies and there is a much larger variety with respect to values and characteristics in manufacture. Therefore, an R-C selective network is resorted to.

The complex poles of a transfer function $H(\omega)$ can be realised by means of an active R-C network[3-30]. When the selective network corresponds to a rejection-band and is placed in the feedback path of an amplifier, the compound network becomes a selective active filter. The choice is made for a Twin-T circuit since it can give transmission zeros on the imaginary axis and therefore will permit, at least theoretically, a complex pole pair with any Q value to be realised.

From the theoretical considerations of measurement, chapter 2, section 3, a bell-shaped $H(\omega)$ filter is required with a low-Q factor. Now, a Twin-T circuit is known to have a characteristic curve similar to a resonant L-C circuit, and hence its form is close to the Gaussian or to a bell-shaped curve when it has a low-Q factor.

Fig. 3.8 shows the symmetrical Twin-T circuit with its source R_s and load R_L impedances. The transfer function is given by[3-31]:

$$H(\omega) = \frac{j\,m}{4 + j\,m} \tag{3.19}$$

where, $m = \omega/\omega_o - \omega_o/\omega$ and the nulling frequency is:

60      $$\omega_o = 1/RC \tag{3.20}$$
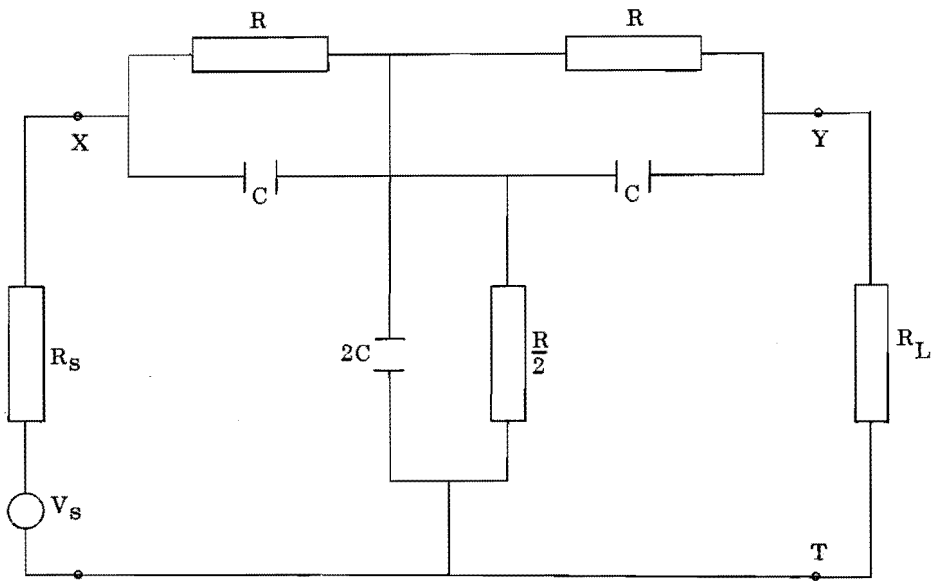
Fig. 3.8 Nulling frequency network using a Twin-T circuit

In order to have an $H(\omega)$ symmetrical around ω_o it is necessary that
the relation $R^2 = 2\,R_s R_L$ be satisfied in the actual circuit[3-32].
When the circuit of the Twin-T is placed in the feedback path of an
amplifier with open-loop gain A_o, and m is small (as happens at fre-
quency values near to the nulling frequency) it can be shown that
the Q of the selective filter is closely calculated from[3-33]

$$Q = \frac{A_o + 1}{4} \qquad\qquad (3.21)$$

If an integrated amplifier is used, we may not be able to realise
the equation $R^2 = 2\,R_s R_L$ since its output impedance is very small
and the needed value of R must be large in order not to have too
large values of capacitance in (3.20) at f_o of 10^{-2} Hz. Consequently,
the input impedance of the operational amplifier must be extremely
high. At the same time the signal must be transferred from the $k\sqrt{\omega}$
filter into the selective filter without affecting the value R_o of
6.5 MΩ in Fig. 3.6 point J.

These difficulties have been avoided by using the circuit of Fig.
3.9. It consists essentially of a high input impedance, unity gain, 61

amplifier stage T_1-T_2 and of a differential stage T_6-T_7, with a selective Twin-T circuit in one of the feedback loops. The output is via an emitter follower T_9.

The input Darlington pair is biased by a potential divider R_1-R_2 of low noise and special carbon APKD resistors. The input impedance at point J is adjusted so as to have the right value to replace the resistor R_o of Fig. 3.6, which permits a direct coupling of the signal.

The operating input base current of $T_1 \leq 10$ nA and the compound transistor pair is temperature stabilised doubly. This is done by slightly draining off part of the base current of T_2[3-34] and secondly, by an overall d.c. feedback through the bleeding resistor R_3. The latter is connected across points of practically the same d.c. potential level by means of the potentiometer R_{13}. Temperature variations between T_1 and T_2 are reduced by enclosing both transistors under a common polysterene cap[3-35]. Polysterene is a resin which has the property of being a very good temperature conductor and a very high electrical insulator.

Transistors T_6-T_7 are a matched pair within 3% for β values at equal V_{BE}. Equal base-emitter voltages are obtained by adjusting the potentiometer R_5. The transistors are mounted together with T_8 on the same crystal chip (BFX-16).

The gain of the differential stage is stabilised by the collector-to-base feedback of T_7 via T_9. A stable d.c. zero output level is obatined at point L of potentiometer R_{12} with an output impedance of approximately 330 Ω. Capacitor C_1 determines the bandwidth from d.c. to 85 Hz for the differential stage while C_o affects the overall response of the circuit of Fig. 3.9 only for frequencies greater than 60 Hz, reducing the contribution of the high frequency side-tail in the selective filter. All resistors are of the 1%, low noise, 150 ppm/^{o}C, thin metal film type.

R being equal to 4 MΩ in Fig. 3.8 and R_s equal to 27 kΩ in Fig. 3.9, the R_L needed for a symmetrical characteristic curve of the Twin-T circuit is well approximated by the input impedance of the Darling-

ton pair T_4-T_3, which has very large β values at low operating cur-
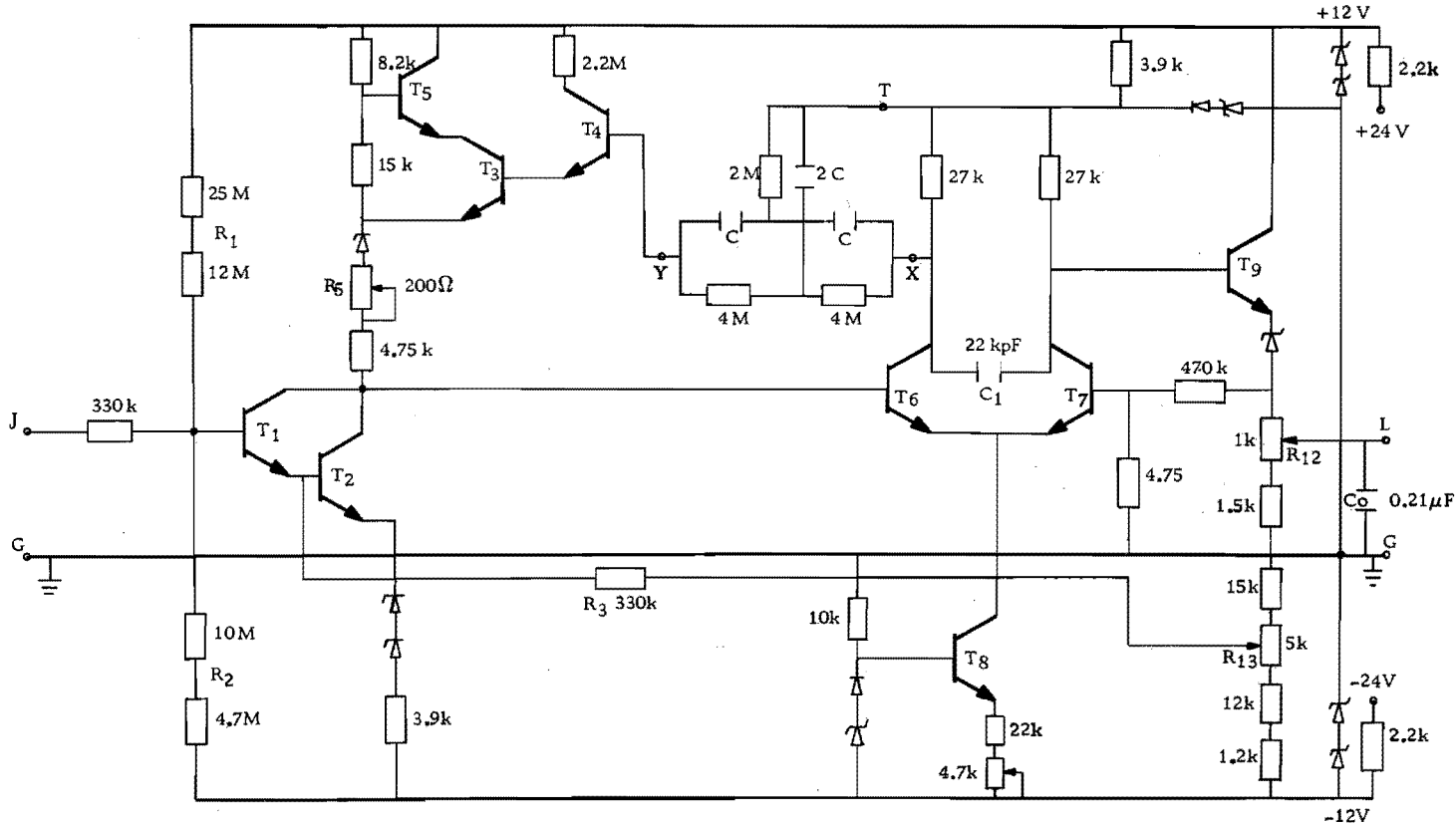
Fig. 3.9   Very-low frequency selective amplifier

rents; the base current of T_4 is 4 nA. Both transistors are operated with low V_{CB} to have a low noise contribution according to equation (3.16) and are enclosed in a common polysterene cap against temperature changes.

The Twin-T circuit has fixed equal resistor R values of 4 MΩ within 10^2 ppm, the resistors being of the 1/4 W, metal film type and having a temperature coefficient of 25 ppm/°C. The capacitors C are made of polysterene or of mica with values realised within 10^{-5} of the required ones by equation (3.20) for the desired spot frequencies. Their leakage current, of the order of 10^{-12} A, is completely negligible. The selective frequency is obtained by exchanging the capacitors (as suggested in chapter 2, section 7) by means of a four-section ceramic switch; all are placed immediately underneath the circuit arrangement of Fig. 3.9. To avoid possible leakage currents owing to humidity a container of silica gel is provided to keep the atmosphere dry.

It was noticed that, owing to the complex wiring of the selective switch, for equal input conditions the amplitude of the selectivity curve decreased slightly as the selective frequency was increased above 2 Hz. The cause seemed to be the parasitic capacitance between several points of the Twin-T circuit, increasing the actual value of C by C_p. Indeed, according to this assumption a constant amplitude of the selectivity curve was obtained by decreasing successively R/2 of Fig. 3.8 by an amount R'/2, within the frequency range 2 to 20 Hz. In Fig 3.10 the resistors $R_1/2$ and $R_1'/2$ are in series and their values, as given in the table below, verify the relation $(R_1 + R_1')/2 = .(R - R')/2$. The value of C_p appeared to be 85 pF and this correction method showed to be very efficient in practice.

The constant voltage gain of the network of Fig. 3.9 gives a constant Q value to the frequency response curve of each filter. Experimentally the value of Q was set equal to 5 and the frequency response followed well a symmetrical curve centered at $f_o = \sqrt{f_1 f_2}$, where f_1 and f_2 are the down 3 dB points.

64

The bank Twin-T network is shown in Fig. 3.10. The following values
of resistors and capacitors were used:

			R	4.000	MΩ				$R_1/2$	1.931	MΩ
f_1	0.010	Hz	C	3.9788	µF	2C	7.9590	µF	$R_1'/2$	83.56	kΩ
f_2	0.0215	Hz		1.8468	µF		3.6938	µF		83.40	kΩ
f_3	0.0464	Hz		0.85777	µF		1.7140	µF		83.10	kΩ
f_4	0.10	Hz		0.39793	µF		0.79585	µF		82.60	kΩ
f_5	0.215	Hz		0.18478	µF		0.36923	µF		82.56	kΩ
f_6	0.464	Hz		85.732	kpF		171.52	kpF		82.48	kΩ
f_7	1.00	Hz		39.775	kpF		79.580	kpF		82.45	kΩ
f_8	2.15	Hz		18.500	kpF		36.970	kpF		76.51	kΩ
f_9	4.64	Hz		8.5875	kpF		17.160	kpF		55.37	kΩ
f_{10}	10.0	Hz		3.9820	kpF		7.9640	kpF		26.93	kΩ
f_{11}	19.8	Hz		1.9925	kpF		3.9835	kpF			
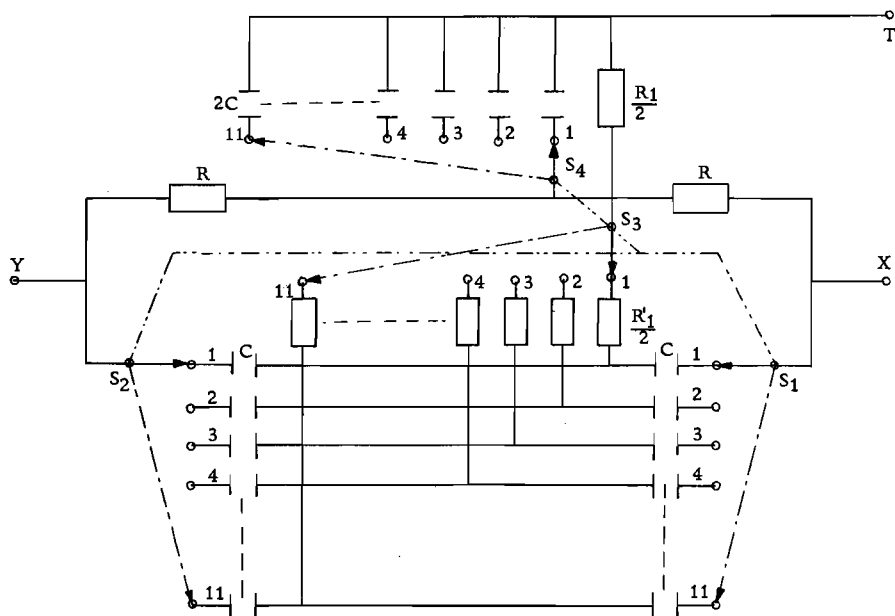
Fig. 3.10   Bank of filters using a Twin-T circuit with the selective
switch S_1-S_2-S_3-S_4

5. Block 5: Main amplifier

The circuit of Fig. 3.11 shows the selective gain amplifier based
on an integrated operational amplifier, RC709D, the gain of which
is very large. The operational amplifier is connected as a non-in-
verting amplifier with an R_F feedback resistor of 56 kΩ. The volt-
age gain of the circuit is given closely by:

$$A_v = 1 + R_F/R_2'$$

(3.22)

where R_2' is the parallel combination of R_2 and the input differen-
tial impedance R_{in} of the amplifier.
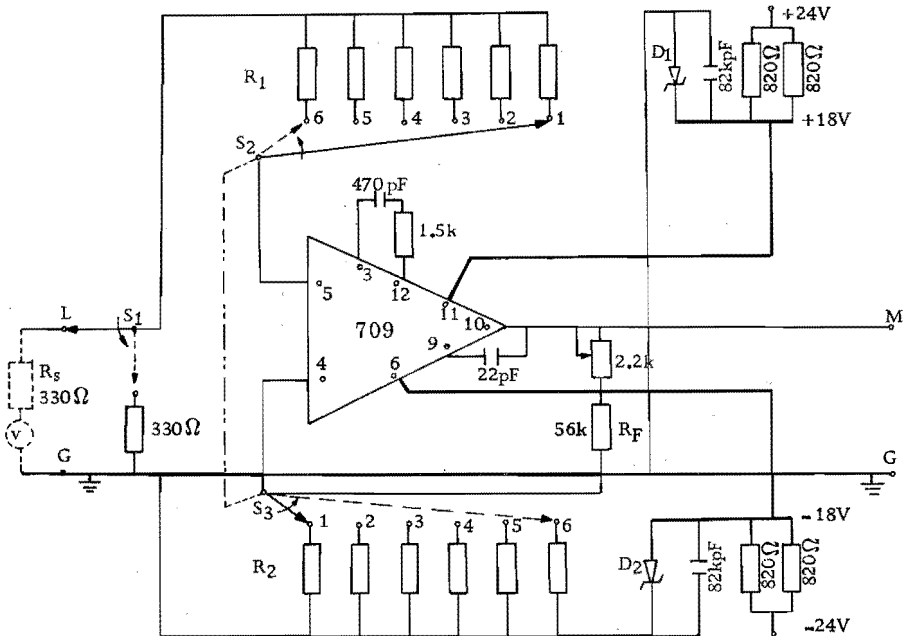
Fig. 3.11 Main amplifier with selective gain adjusted by switch
S_2-S_3

Now, once the desired voltage gain A_v is chosen, the required R_2 may
be calculated from (3.22). The source impedance of the inverting in-
put R_{s_2} is the parallel combination of R_F and R_2. Then a source im-
pedance $(R_{s_1} = R_1 + R_s)$ at the non-inverting input equal to R_{s_2} is
introduced in order to reduce the input differential drifts.

The input signal at terminals L and G is taken from a zero d.c. po-
tential level and a source resistance R_s of 330 Ω at the output of
block 4. By adjusting the potentiometer of 2.2 kΩ on the feedback
path, a zero d.c. output level is obtained at point M.

The actual voltage gains A_{v_i}, i from 1 to 6, are:

  A_v: 2.0 ; 5.0 ; 7.5 ; 10.5 ; 21.0 ; 31.5.

A_{v_i} is selected by means of the switch S_2-S_3, which simultaneously
connects the values of R_1 and of R_2.

The bank of resistors R_1 and R_2 have small bias currents, are of met-
al film type, and have a very low noise voltage, viz. 0.1 µV/V. The
operational amplifier is frequency compensated to have a flat band
response from d.c. to 100 Hz.

The object of switch S_1 is to disconnect the input signal which may
have large transients when the selective frequency of the filter is
changed, since then the charged capacitors of the Twin-T circuit are
replaced by other capacitors.

Taking into account the specified input differential impedance R_{in}
of 400 kΩ and equation (3.22), we find the values of R_{1i} and R_{2i}
within 10^{-4} to be as follows:

A_{v1}	R_{11}	27.710 kΩ	R_{21}	56.100 kΩ	
A_{v2}	R_{12}	11.250 kΩ	R_{22}	14.500 kΩ	
A_{v3}	R_{13}.	7.860 kΩ	R_{23}	9.557 kΩ	
A_{v4}	R_{14}	5.380 kΩ	R_{24}	6.310 kΩ	
A_{v5}	R_{15}	2.516 kΩ	R_{25}.	2.977 kΩ	
A_{v6}	R_{16}	1.576 kΩ	R_{26}	1.941 kΩ	

6. Block 6: Selective low-pass filter

The bell – shaped characteristic curve of a Twin-T circuit when fed back has tails extending over several decades. Therefore, according to the considerations of chapter 2, section 3, we introduce a low-pass filter with cut-off frequency 4 ω_o in order to decrease the contribution of the high frequency tail in the main filter centered at ω_o.

For an operational amplifier with a very large voltage gain A_v and high input differential impedance, the transfer function $H(\omega)$ of the circuit of Fig. 3.12 can be shown to be given by[3-36]:

$$H(\omega) = \frac{- A_v \omega_o'^2}{s^2 + a\omega_o's + \omega_o'^2} = - \frac{1}{R_1 R_3} \cdot 1 \Big/ \left(s^2 C_1 C_2 + s C_1 (1/R_1 + 1/R_3 + 1/R_2) + \right.$$

$$\left. + 1/R_2 R_3 \right) \qquad (3.23)$$

where A_v is the voltage gain of the circuit, $s = j\omega$ and ω_o' is the cut-off frequency from which the roll-off response is 40 dB/decade.
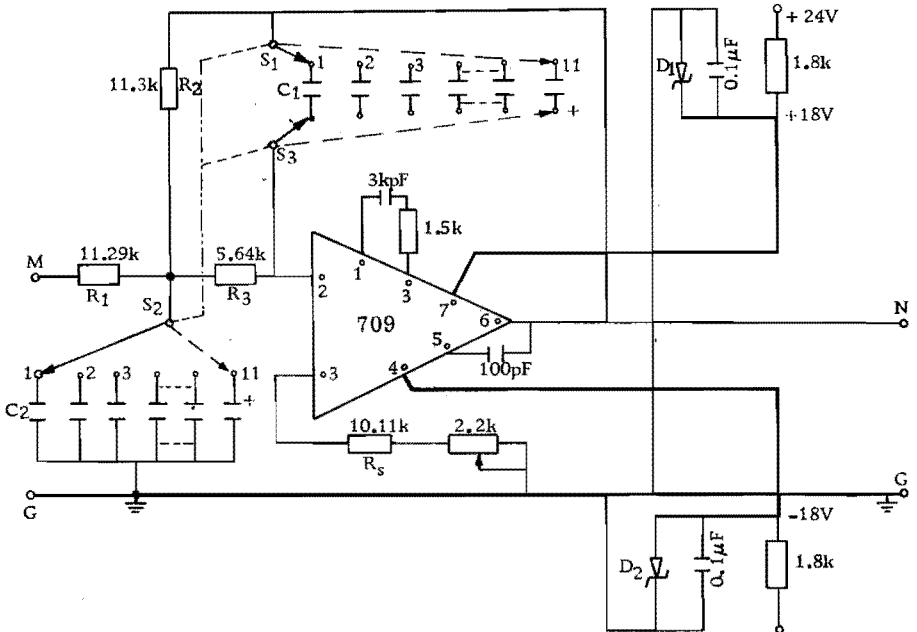
Fig. 3.12   Low-pass active filter with selective switch S_1-S_2-S_3

Now, choosing

$$C_1 = k/\omega_o'$$ (3.24)

equation (3.23) yields:

$$C_2 = 4/a^2.(A_v+1)C_1; \quad R_1 = a/2kA_v; \quad R_2 = a/2k = R_1 \cdot A_v;$$

$$R_3 = a/2k(A_v+1)$$ (3.25)

and the filter shows to have a maximally flat band response for $a=\sqrt{2}$.

A source resistor $R_s = R_3 + R_2//R_1$ is placed at the non-inverting input, for the elimination of the d.c. drifts. The potentiometer of 2.2 kΩ in series with R_s allows to obtain a zero d.c. level output. The selected ω_o' values are obtained by the use of switch $S_1-S_2-S_3$ which simultaneously varies the values of C_1 and C_2.

Now, let us choose the following parameter values;

$$f_o = 20 \text{ Hz}; \quad f_o' = 4f_o; \quad C_1 = 0.125 \text{ }\mu\text{F}; \quad A_v = 1; \quad a = \sqrt{2}.$$

Then, from the set of equations (3.27) and (3.28) we obtain:

$$R_1 = R_2 = 11.275 \text{ k}\Omega, \quad R_3 = 5.637 \text{ k}\Omega, \quad C_2 = 0.50 \text{ }\mu\text{F}.$$

The following values of C_1 and C_2 were realised with tantalum and polysterene capacitors in the bank of low-pass filters of Fig. 3.12:

f_1	0.01	Hz	actual	f_1'	0.0373	Hz	C_{1-1}	1010	μF	C_{2-1}	251.0 μF
f_2	0.0215	Hz		f_2'	0.0819	Hz	C_{1-2}	468.0	μF	C_{2-2}	116.1 μF
f_3	0.0464	Hz		f_3'	0.176	Hz	C_{1-3}	215.0	μF	C_{2-3}	53.85 μF
f_4	0.10	Hz		f_4'	0.387	Hz	C_{1-4}	99.7	μF	C_{2-4}	24.8 μF
f_5	0.215	Hz		f_5'	0.83	Hz	C_{1-5}	46.1	μF	C_{2-5}	11.58 μF
f_6	0.464	Hz		f_6'	1.79	Hz	C_{1-6}	21.55	μF	C_{2-6}	5.38 μF
f_7	1.0	Hz		f_7'	4.01	Hz	C_{1-7}	10.00	μF	C_{2-7}	2.49 μF
f_8	2.15	Hz		f_8'	8.48	Hz	C_{1-8}	4.68	μF	C_{2-8}	1.167 μF
f_9	4.64	Hz		f_9'	18.5	Hz	C_{1-9}	2.17	μF	C_{2-9}	0.537 μF
f_{10}	10.0	Hz		f_{10}'	40.0	Hz	C_{1-10}	1.00	μF	C_{2-10}	0.248 μF
f_{11}	19.8	Hz		f_{11}'	79.4	Hz	C_{1-11}	0.50	μF	C_{2-11}	0.125 μF

7. Block 7: Analogue multiplier

A commercial solid-state unit was used, M 101 of Intronics, which operates on a pulse-height pulse-width principle. It has its own internal clock frequency of 25 kHz and can take inputs of $\pm$ 10 volts; the output has a 10^{-1} attenuation constant.

Both input impedances are larger than 75 kΩ and yield a linearity better than 0.25%. This linearity is defined as the maximum deviation from the best straight line divided by the full scale value. For an output voltage of 20 Vpp, the frequency response is flat within $\pm$ 1% from d.c. to 300 Hz and down 3 dB at 1 kHz.

The output drift is $\pm$ 0.5 mV/^{o}C max., while a small amount of output ripple and noise exists, owing to the clock frequency signal; however, the output ripple is only 1 mV max. pp from 5 Hz to 1 kHz. The d.c. offset level is smaller than $\pm$ 10 mV for zero inputs.

8. Block 8: Hybrid integrator-averager

The integration is performed by an analogue-digital converter (A-D) and an electronic counter.

As analogue-digital converter was used a type M 651 Beckman voltage-to-frequency converter. The output pulse frequency is precisely proportional to the d.c. input voltage and has an almost instantaneous response to changes in input voltage. Therefore, the output frequency accurately follows the variations of the input voltage.

The A-D converter has full-scale sensitivities of 0.1, 1.0, 10, 100, and 1000 V d.c., yielding a 0 to 100 kHz pulse output for full scale sensitivity, and for both input polarities without switching. Its linearity is better than $\pm$ 0.02% of full scale and its input may still be increased by approximately 30% above full scale with an output accuracy of $\pm$ 0.15%. The input impedance is 100 kΩ for 0.1V d.c. input range and 1 MΩ for all other ranges. A d.c. blocking tantalum capacitor of 340 μF was placed at the input of the A-D converter to eliminate the d.c. output offset of the multiplier.

The electronic counter used was a 3734A Hewlett-Packard instrument
70 with five digits display to which a six digit electro-mechanical

counter was connected to count the number of times the electronic counter saturates.

A stop-clock records the measuring time T prescribed by the theoretical considerations. The electronic mechanical counter result is divided by T and the bandwidth $\Delta\omega_o$ at the end of each prescribed frequency ω_o measurement. Thus, a quantity is obtained which is proportional to the average noise power density centered at ω_o.

MEASUREMENTS AND ANALYSIS OF LOW-FREQUENCY NOISE

(A) Flicker Noise in Resistors

1. Experimental state of art

Bernamont in 1934 was the first observer of noise in excess of thermal noise and which was generated in certain resistors with a steady current through them[4-1]. When the current flows, fluctuations of voltage or current of relatively small amplitude, but with a very uneven distribution, appear at the terminals of the resistor. This phenomenon is normally referred to as current noise or flicker noise.

Experimental results have commonly shown that the spectral density of the current noise is given by the relation:

$$S(\omega) = k \ I^{\alpha} \ \omega^{-\beta} = k' \ V^{\gamma} \ \omega^{-\beta} \tag{4.1}$$

where k and k' are constants, I is the d.c. current, V is the d.c. applied voltage, ω is the angular frequency of measurement. The exponents α, γ and β are parameters. If Ohm's law is valid here, $\alpha = \gamma$. Most investigators[4-1 - 4-10] have found experimentally the value 2 for α and γ in carbon resistors operated at low-current levels. As to the value of β, there seems to be no agreement. Table 4-I contains a historical view showing a spread of the β value from 0.6 to

1.4 for carbon resistors in the low frequency range 10^{-4} Hz to 1 kHz.

Table 4-I

Investigator:	Year:	Value of α:	γ:	β:	Freq. Range:
Bernamont[4-1]	1934	2, low current	2	0.88-1.1 low freq. 2, high freq.	96Hz-162kHz
Otto[4-2]	1934		2	1-1.4	5Hz-1kHz
Meyer and Theide[4-3]	1935	2	2	1-2	
Christensen and Pearson[4-4]	1936		1.75-1.9	1	50Hz-10kHz
Abson, Harris and Roberts[4-5]	1946	1.7-1.9		1	0.3Hz-500Hz
Campbell and Chipman[4-6]	1948	2		1.1 low freq. 1.7 high freq.	10kHz-500kHz
Templeton and MacDonald[4-7]	1953	2		1.01	$2.5 10^{-4}$ Hz- 7.5Hz
Van Vliet, Van Leeuwen, Blok and Ris[4-8]	1954	2		1-1.1	10kHz-1MHz
Kirby[4-9]	1959		1.4-2.2	0.6-1	250Hz-200kHz
Brophy[4-10]	1965	2		1.02	8Hz-10kHz

2. Considerations on measurements

We too have also done measurements on carbon-film resistors and found fluctuations with time in the parameter β in each individual resistor measured and operated at very low current levels. It was thought that such an operating mode would allow the appearance of relevant features which may be obscured at higher current levels.

In addition to the non-constancy of β, some resistors have a very un-stable noise with frequent bursts of noise during short periods of time which cannot be considered as normal fluctuations[4-6, 4-8, 4-9]. Campbell and Chipman[4-6], when measuring carbon resistors, found sim-ilar bursts at 150 kHz, but is was not possible for them to deter-mine if the abnormal fluctuations were simultaneously present at   73

different frequencies. Recently, Williams and Burdett[4-11] found that randomly spaced pulses were often superimposed on the statistically regular current noise in cermet resistor films.

The relative output-noise power density $\omega \cdot S(\omega)$ was measured for 10 MΩ carbon resistors with a direct current of 1 µA. Fig. 4.1 shows the measurements carried out with a desired statistical error ε from 2% at a spot frequency of 20 Hz to 7.5% at 0.01 Hz. It took almost three days to measure this spectrum range.
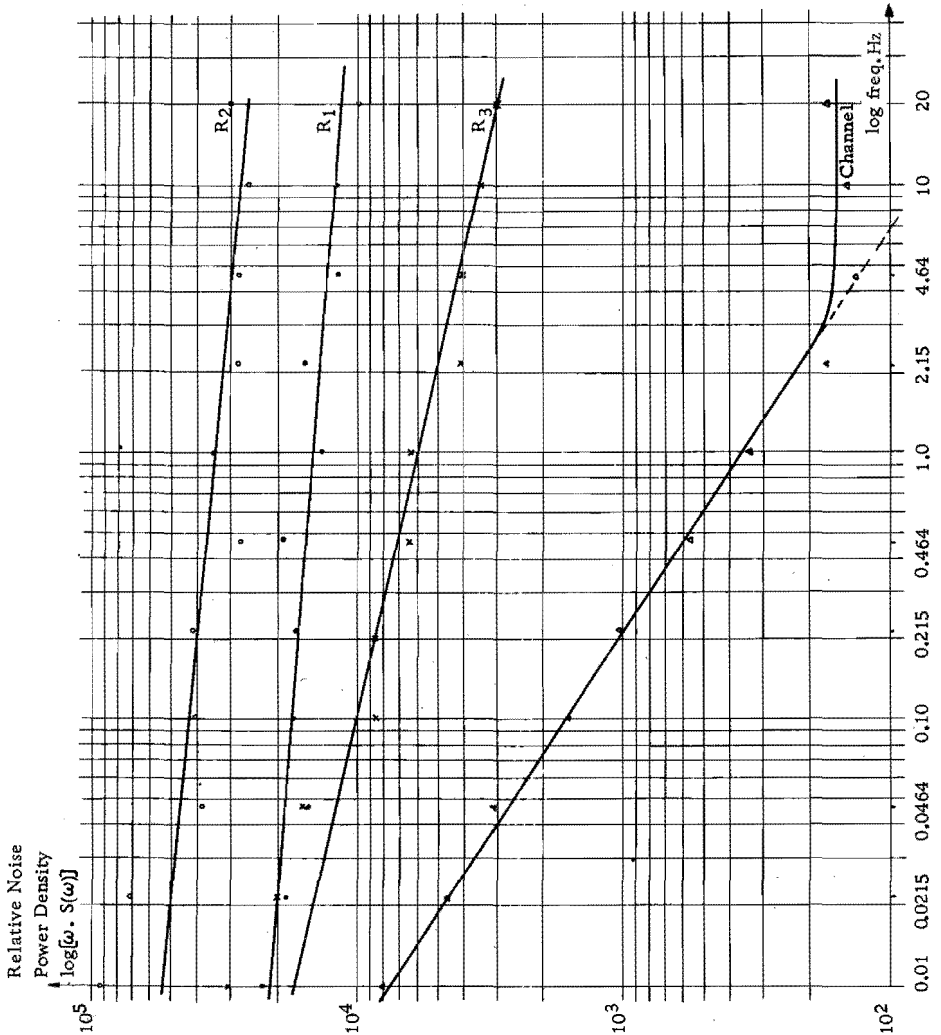

Fig. 4.1   Relative noise power density spectrum of the measuring channel and of the resistors R_1, R_2, R_3

First, the noise power density of the channel was measured. It is seen to have a white noise spectrum down to 3 Hz and then follows the $\omega^{-\beta}$ law with β equal to 1.68. At 3 Hz the channel has an equivalent noise resistance R_n of 25 kΩ at room temperature and for unity bandwidth.

A straight line fits the eleven spectral points of each of the three measured resistors R_1, R_2 and R_3, when plotted on a log-log scale indicating an input spectrum of the type:

$$S(\omega) = K\, \omega^{-\beta} \qquad 1.09 < \beta < 1.22 \qquad\qquad (4.2)$$

The resistors R_1, R_2, R_3 were chosen for being especially noisy samples.

Nevertheless, some points in Fig. 4.1 appear to deviate from the best straight line by much more than the allowable $\pm\, 2\,\epsilon$, mainly at the lowest frequencies. It seems we are dealing with fluctuations of fluctuations.

From the theoretical point of view, Mandelbrot[4-12] has shown that functions can be constructed from random repeatable sequences to have a spectral density of the type $\omega^{-\beta}$, $0 \leq \beta \leq 2$, which behave more erratically in time than is expected from functions subjected to the Wiener-Khintchine theorem. When averaged over a long time, these functions do not have a Gaussian distribution, and extreme values have a high probability of occurrence, although the marginal distribution of the function may itself be Gaussian.

Indeed, noise measurements on the above cracked-carbon film resistors taken during long periods of time have shown a current noise fluctuating randomly between a high and a low noise level, and having a non-Gaussian distribution. Therefore, it appeared clearly from the above considerations and from the presence of bursts that, if the noise mechanism belonged to a quasi-stationary process, it would be necessary to measure a shorter spectrum range in a shorter time in order to be able to measure the noise during the same operating mode and excitation state of the sample under investigation.

Table 4-II

Measurement, N°	Time of Measurement, hour	Relative Output Noise Power Density: $\omega.S(\omega)$						Slope at output, $\beta-1$	%, ε Statistical Error	%, Max. Deviation from straight-line
		20cs	10.0cs	4.64cs	2.15cs	1.0cs	0.46cs			
1	1^{st}h	67	90	104	119	156	147	0.20	9.49	14.8
2	3^{rd}h	141	155	157	235	293	337	0.27	9.33	18.7
3	4^{th}h	70	63	89	113	164	190	0.31	14.57	22.0
4	5^{th}h	68	57	87	105	138	170	0.28	13.58	21.4
5	6^{th}h	56	83	100	188^+	367^+	566^+	0.64	16.07	27.0
6	22^{th}h	49	64	88	210^+	171^+	326^+	0.54	24.88	40.2
7	24^{th}h	146	160	164	283	356	368	0.32	16.28	22.80
8	27^{th}h	47	58	87	90	150	163	0.32	10.51	15.46
9	28^{th}h	66	81	116	173^+	335^+	261	0.46	23.01	35.45

Time T needed for | 10%: 16.05s 31.83s 1m8.6s 2m28.05s 5m18.3s 11m26s
statist. error ε | 2%: 7m 3s 13m16s 28m35s 1h1m14s 2h12m38s 4h45m50s   (+): see text.

3. Quasi-stationary noise in resistors

The relative output noise power density $\omega.S(\omega)$ for nine consecutive measurements on the same resistor R_2 of Fig. 4.1, taken within 28 hours with a desired ε of 10%, is shown in Table 4-II. Taking into account the waiting time required between two measurements at different frequency values, so that the switching transients have died out, a measuring time of 3/4 h was needed for each row of the spectrum range. The values with an asterisk indicate that considerable burst noise was observed during that measurement. A straight line to fit the noise power data, plotted on a log-log scale, was obtained by taking the average value of two groups of ordinates since the abscissae are equidistant, and the line had a slope of the value $\beta -1$.

Taking Table 4-II as a guide, we may conclude the following. There are two groups of measurements. The first contains the measurements 5, 6 and 9. They show a non-stationary behaviour because bursts were observed during measuring, and they have large deviations from the straight line resulting in a non-Gaussian distribution, as is apparent from the last two colums. The second group is formed by the other measurements, which are much closer to what may be expected from a

statistical Gaussian distribution and correspond to stationary peri-

$$S(\omega) = K\omega^{-\beta}$$

Line 7	Slope	= 1.32
3		= 1.31
2		≐ 1.27
4		= 1.28
8		= 1.32
1		= 1.20
5		= 1.64
6		= 1.54
9		= 1.46
10		= 0.80
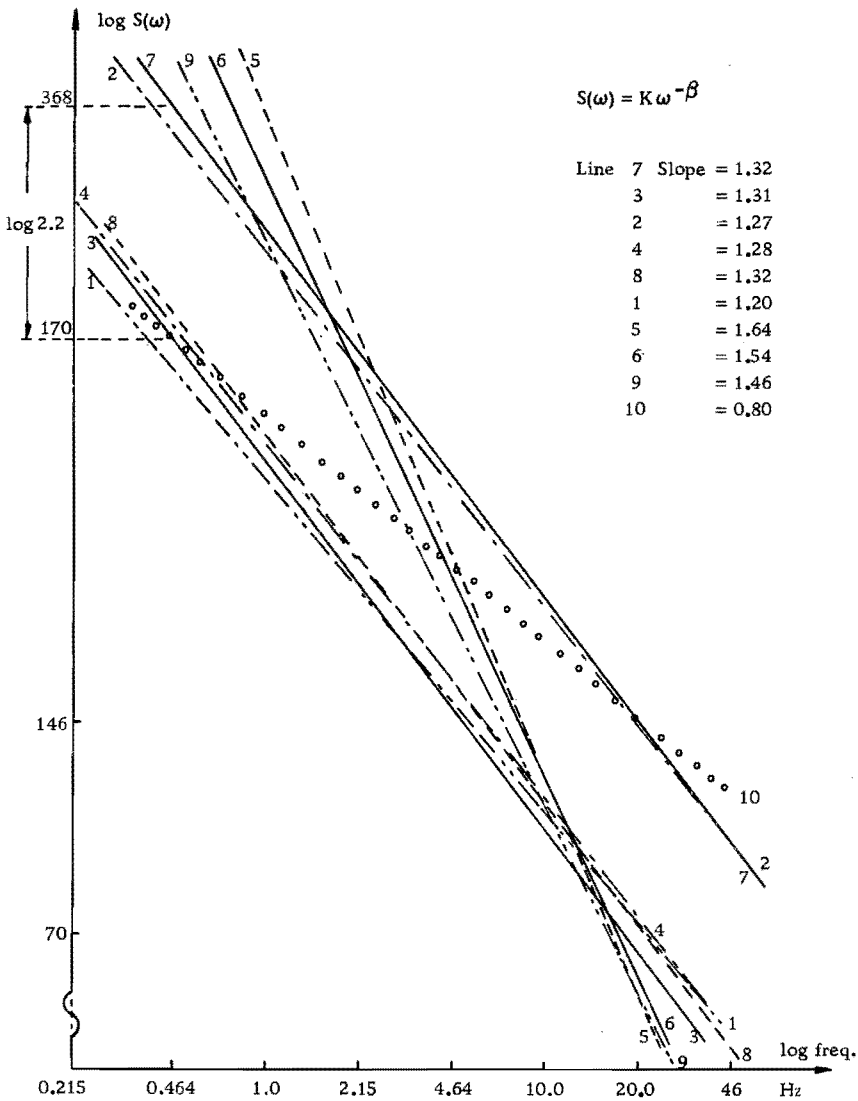
Fig. 4.2   *Nine consecutive measurements of current-noise spectrum density as functions of frequency for the carbon resistor R_2, 10 MΩ, with 1 µA d.c.*

ods of noise with a slope of 1.28 ± 0.05. Thus its noise spectrum is given by $S(\omega) = K\,\omega^{-1.28}$, where K may vary by a factor greater than two. The other two sample resistors, R_1 and R_3, had a β of 1.20 and 1.12 with K values varying by a factor 2 and 1.4, respectively.

The noise-power data of Table 4-II are plotted in Fig. 4.2 on a log-log scale. Each measurement is represented by its best straight line **77**

with its equivalent input slope. It is clear from Fig. 4.2 that there are at least two states of excitation and that the noise power density fluctuates between a high and a low level. Now, if large bursts occurred only during the high-frequency measurements, which is less probable since less measuring time is needed than for low frequencies, a feasible spectrum would have $\beta \simeq 0.8$ (line 10). Hence, the sample in question would have a spread of β from 0.8 to 1.64. This spread agrees with that given in Table 4-I and indicates a difficulty encountered when repeating low-frequency noise measurements. The above considerations were published by the author before[4-13].

Malakof[4-14] has already considered the possibility of flicker noise being quasi-stationary while following the law of equation (4.1), and concluded that apparently flicker noise can be considered a random non-stationary process with stationary increments. But unfortunately no measurements were carried out under this scope.

More recently, Brophy has studied the probability amplitude distribution of 1/f noise and of Nyquist noise in carbon resistors within the range of 8 Hz to 10^4 Hz [4-15]. Brophy found that both types of noise obey a normal distribution law in all the sampling time intervals investigated. But in the case of 1/f noise, the variance of the distribution itself fluctuates in identical sampling intervals. This means that 1/f noise is not stationary in the usual statistical sense such as is true for Nyquist or thermal noise, but rather possesses a weaker form of stationarity.

Brophy himself points out that his experimental technique[4-16] tends to yield greater variance fluctuations in 1/f noise signals than in

Nyquist noise signals. This is so because large low-frequency components characteristic of 1/f noise introduce a correlation between successive sampling intervals. Hence, during the same measuring time T there are fewer independent samples in the case of 1/f noise compared to Nyquist noise, which has a white noise-power spectrum. Statistical fluctuations associated with fewer independent samples tend to cause variations in experimentally determined variances. With our

78 experimental technique (see chapter 2, section 4) of prewhitening

the noise before analysing it we avoid the above correlation intro-
duced by the low-frequency components and, consequently, the statis-
tical fluctuations due to fewer independent samples; nevertheless,
we still obtain fluctuations in the output noise-power density spec-
trum.

Furthermore, assuming that the spectral density of the fluctuations
of the variance is constant, as should be for a stationary process,
the variance of the variance should decrease with the measuring time
T as $1/T$ [4-17]. But this was not observed in the measurements perform-
ed by Brophy[4-15], while we found the following. For the same resis-
tor R_2 as above, the noise power density also fluctuated by a factor
2 during consecutive and identical sampling intervals (now taken for
an ε of 2%) and at the same frequency. Thus, the increase of time T
did not decrease the fluctuating factor 2.

Therefore, we conclude that in some carbon resistors 1/f noise is
quasi-stationary, the cause of which may be found in the observed
random bursts that change the noise excitation state of the carbon
resistor.

(B) Burst Noise in Transistors
4. Analysis

The spontaneous fluctuations of current have obtained special inter-
est among the various random noise phenomena that appear in semicon-
ductor devices. These spontaneous bursts consist of a series of cur-
rent pulses with constant amplitude and with pulse lenghts distrib-
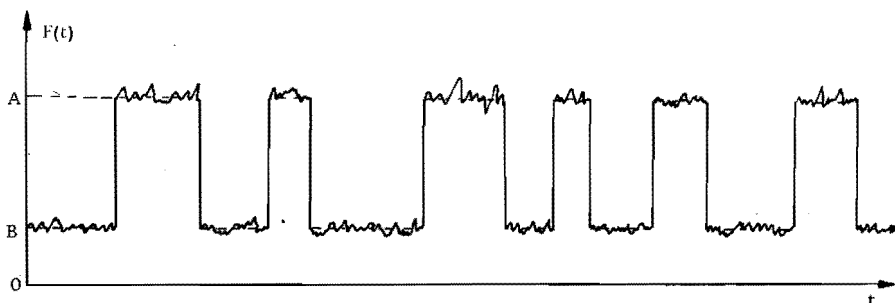

Fig. 4.3   A random telegraph signal

uted statistically. Hence, they are classified as a random telegraph
signal, Fig. 4.4, with an extra noise component superimposed.

In the following pages we shall be concerned with obtaining the
noise-power density spectrum of the random signal of Fig. 4.3. First,
we consider the random telegraph signal alone (Fig. 4.4), and sec-
ondly we take into consideration the additional superimposed noise
component.
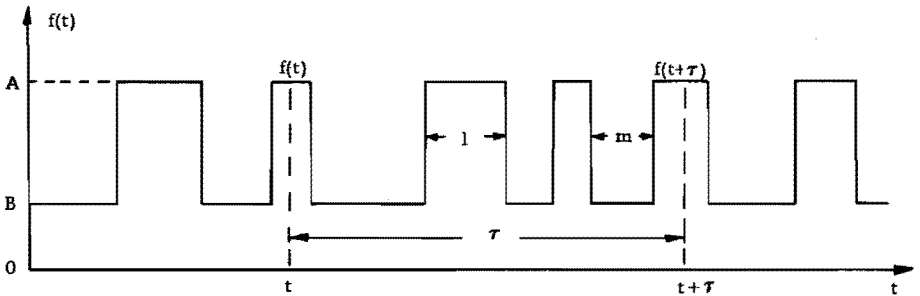
Fig. 4.4   Unsymmetrical random telegraph signal between levels B
            and A

4.1 Unsymmetrical random telegraph signal

It has been observed experimentally that for most transistors, in
which burst noise is found, their random telegraph signal is not a
symmetrical one, i.e. when the noise is observed over a long time,
the signal is longer at one d.c. level than at the other. We know,
also experimentally, that the pulse lenghts have a statistical dis-
tribution very close to a Poisson one. Let us now obtain the noise-
power density spectrum of the noise signal f(t) of Fig. 4.4.

The function f(t) represents the pulse-signal noise which varies
randomly between two discrete levels A and B, with a probability p
of having value A at any time t, and a probability q = 1 - p of hav-
ing value B; the pulse lengths ℓ and m are assumed to have a Poisson
distribution.

We will calculate (a) the autocorrelation function and then (b) its
Fourier transform, which gives the power spectrum density by the
Wiener-Khintchine theorem.

(a) Autocorrelation function

The autocorrelation function of f(t) is given by:

$$R_B(\tau) = \overline{f(t) \cdot f(t+\tau)} \qquad (4.3)$$

Let $P_{AB}(\tau)$ represent the probability of f(t) having at time t + τ the value B once it has had at time t the value A. Then, (4.3) becomes:

$$R_B(\tau) = A\,p \times A\,P_{AA}(\tau) + A\,p \times A\,P_{AB}(\tau) + B\,q \times A\,P_{BA}(\tau) +$$

$$+ B\,q \times B\,P_{BB}(\tau) \qquad (4.4)$$

From Fig. 4.4 we see that, if at time t the function f(t) has an amplitude A, in order to have again the value A at time t + τ, it is necessary that an even number of transitions between its two levels A and B occur during the interval time τ. Therefore, for obtaining $P_{AA}(\tau)$ we must calculate the sum of all probabilities of an even number of transitions during τ, while for $P_{AB}(\tau)$ we need the sum of all probabilities of an odd number of transitions during τ. The same can be said for $P_{BB}(\tau)$ and $P_{BA}(\tau)$, but now starting from level B.

Let us construct our own probability distribution from Fig. 4.4, knowing it is a Poisson type, with the following properties:
(1) If f(t) = A, the probability of having a transition in the time interval (t, t + τ) is μ·dt.
(2) If f(t) = B, the probability of having a transition in the same time interval is η·dt.
Starting at level A, the probability of having no transitions in time τ + δτ, defined as $P_o(t + \delta\tau)$, is:

$$P_o(t + \delta\tau) = P_o(\tau)P_o(\delta\tau) = P_o(\tau)\,(1 - \mu\delta\tau) = P_o(\tau) + \frac{dP_o(\tau)}{d\tau}\,\delta\tau$$

$$(4.5)$$

considering in the last expression the two first terms of a Taylor's **81**

series, and resolving (4.5) we obtain $dP_o(\tau)/P_o(\tau) = -\mu\delta\tau$; the solution of which, knowing that for $\tau = 0$, $P_o(0) = 1$, is:

$$P_o(\tau) = e^{-\mu\tau} \tag{4.6}$$

The probability of one transition in the time $\tau + \delta\tau$, defined as $P_1(\tau + \delta\tau)$, is:

$$P_1(\tau + \delta\tau) = P_o(\tau)P_1(\delta\tau) + P_1(\tau)P_o(\delta\tau) = P_o(\tau)\mu\delta\tau + P_1(\tau) \cdot$$

$$(1 - \eta\delta\tau) = P_1(\tau) + \frac{dP_1(\tau)}{d\tau} \delta\tau \tag{4.7}$$

which yields the differential equation:

$$\frac{dP_1(\tau)}{d\tau} + \eta P_1(\tau) = \mu P_o(\tau) \tag{4.8}$$

and knowing that for $\tau = 0$, $P_1(0) = 0$, the solution of (4.8) is:

$$P_1(\tau) = \frac{\mu}{\eta-\mu} e^{-\mu\tau} - e^{-\eta\tau} \tag{4.9}$$

In general, neglecting the probabilities of having 2, 3, ...n transitions during the time $\delta\tau$, the probability of having n transitions in $\tau + \delta\tau$, defined as $P_n(\tau + \delta\tau)$, is:

for <u>n even</u> $\quad P_n(\tau + \delta\tau) = P_n(\tau) (1 - \mu\delta\tau) + P_{n-1}(\tau) \eta\delta\tau \tag{4.10}$

and

for <u>n odd</u> $\quad P_n(\tau + \delta\tau) = P_n(\tau) (1 - \eta\delta\tau) + P_{n-1}(\tau) \mu\delta\tau \tag{4.11}$

Equating (4.10) and (4.11) to the two first terms of a Taylor's series and resolving the equality we arrive at:

<u>n even</u>

82

$$\frac{dP_n(\tau)}{d\tau} + \mu P_n(\tau) = \eta P_{n-1}(\tau) \tag{4.12}$$

<u>n odd</u>

$$\frac{dP_n(\tau)}{d\tau} + n P_n(\tau) = \mu P_{n-1}(\tau) \tag{4.13}$$

Now, referring n even and n odd to a common n considered as an even number, we may write (4.13) as:

<u>n odd</u>

$$\frac{dP_{n-1}(\tau)}{d\tau} + n P_{n-1}(\tau) = \mu P_{n-2}(\tau) \tag{4.14}$$

Differentiating again (4.12) and substituting in it the expressions of $P_{n-1}(\tau)$ and $dP_{n-1}(\tau)/d\tau$ from (4.14) and (4.12) we obtain the recurrent differential equation:

<u>n even</u>

$$\frac{d^2}{d\tau^2} P_n(\tau) + (\mu + n) \frac{d}{d\tau} P_n(\tau) + \mu n P_n(\tau) = \mu n P_{n-2}(\tau) \tag{4.15}$$

which may be expressed with the D operator's form as:

$$\left[D^2 + (\mu + n)D + \mu n \right] P_n(\tau) = \mu n P_{n-2}(\tau) \tag{4.16}$$

Remembering that:

$$P_{AA}(\tau) = \sum_{\substack{n=0 \\ n \text{ even}}}^{\infty} P_n(\tau) \tag{4.17}$$

we sum both members of (4.16) and obtain:

$$\mu n \left[P_0(\tau) + P_2(\tau) + P_4(\tau) \ldots \ldots P_n(\tau) \right] = \left[D^2 + (\mu + n)D + \mu n \right] \times$$

$$\left[P_2(\tau) + P_4(\tau) \ldots \ldots P_{n+2}(\tau) \right] \tag{4.18}$$

As $n \to \infty$, $\displaystyle\sum_{n=2,4\ldots}^{n} P_n(\tau) = \sum_{n=2,4\ldots}^{n+2} P_n(\tau)$ and (4.18) takes the form:

$$\mu n P_0(\tau) = \left[D^2 + (\mu + n)D \right] \sum_{\substack{n=2 \\ n \text{ even}}}^{\infty} P_n(\tau). \tag{4.19}$$

83

Replacing $P_o(\tau)$ by its equivalent (4.6) we arrive at a differential equation the solution of which is of the type:

$$\sum_{n=2,4}^{\infty} P_n(\tau) = M + N e^{-(\mu+\eta)\tau} - e^{-\mu\tau} \tag{4.20}$$

and adding to both sides $P_o(\tau)$, we have:

$$\sum_{\substack{n=0 \\ n \text{ even}}}^{\infty} P_n(\tau) = M + N e^{-(\mu+\eta)\tau} \tag{4.21}$$

The constants M and N are calculated from the knowledge of $\sum_{n=0,2...}^{\infty}(0)$

$= 1$ and $\sum_{n=0,2...}^{\infty}(\infty) = p$, i.e. the sum of probabilities of always having a value A. The final result is:

$$P_{AA}(\tau) = \sum_{\substack{n=0 \\ n \text{ even}}}^{\infty} P_n(\tau) = p + (1 - p)e^{-(\mu + \eta)\tau} \tag{4.22}$$

Equation (4.22) gives the sum of all probabilities of having an even number of transitions in an interval of time τ, having started at level A.

Since at time $t + \tau$ the signal is either at level A or B, we have:

$$P_{AB}(\tau) = 1 - P_{AA}(\tau) \tag{4.23}$$

Then, using the expression of (4.22) we arrive at:

$$P_{AB}(\tau) = \sum_{\substack{n=1 \\ n \text{ odd}}}^{\infty} P_n(\tau) = q - q e^{-(\mu + \eta)\tau} \tag{4.24}$$

Equation (4.24) gives the sum of all probabilities of having an odd number of transitions in an interval of time τ, having started at level A.

84 level A.

By analogous reasoning, having started at level B, we have:

$$P_{BB}(\tau) = \sum_{\substack{n=0 \\ n \text{ even}}}^{\infty} P_n(\tau) = q + (1 - q)e^{-(\mu + \eta)\tau} \tag{4.25}$$

$$P_{BA}(\tau) = \sum_{\substack{n=1 \\ n \text{ odd}}}^{\infty} P_n(\tau) = p - p\, e^{-(\mu + \eta)\tau} \tag{4.26}$$

Therefore, introducing into (4.4) the sum of the probabilities given by (4.22), (4,24), (4,25) and (4,26), we obtain the autocorrelation function of the burst-pulse signal noise f(t) of Fig. 4.4, given by:

$$R_B(\tau) = A^2 p(p+q\, e^{-(\mu+\eta)|\tau|}) + AB\, pq(1-e^{-(\mu+\eta)|\tau|} + BA\, qp \times$$

$$(1-e^{-(\mu+\eta)|\tau|}) + B^2 q(q+p\, e^{-(\mu+\eta)|\tau|}) = (Ap + B\, q)^2 +$$

$$(A - B)^2 p\, q\, e^{-(\mu+\eta)|\tau|} \tag{4.27}$$

For the particular case of level B being zero, we have:

$$R_B(\tau) = A^2 p\ (p + q\, e^{-(\mu+\eta)|\tau|}) \tag{4.28}$$

Equation (4.28) is the autocorrelation function of the unsymmetrical random telegraph signal for one level; and for the case of a symmetrical one, $p = q = 1/2$ and $\mu = \eta$, which reduces (4.28) to:

$$R(\tau) = \left(\frac{A}{2}\right)^2 \cdot (1 + e^{-2\mu|\tau|}) \tag{4.29}$$

and agrees with the result of the autocorrelation function of the Poisson rectangular wave, which appeared for the first time in the work of Kenrick[4-18].

(b) Power Spectrum $S(\omega)$

The power density spectrum is given by the following Fourier transform:

$$S(\omega) = \frac{1}{2\pi} \int_{-\infty}^{\infty} R(\tau)\, e^{-j\omega\tau}\, d\tau \tag{4.30}$$

Then, replacing $R_B(\tau)$ by (4.27) we obtain:

$$S(\omega) = \frac{1}{2\pi} \int_{-\infty}^{\infty} (Ap+Bq)^2 e^{-j\omega\tau} d\tau + \frac{1}{2\pi} \int_{-\infty}^{\infty} (A-B)^2 pq e^{-(\mu+\eta)|\tau|} e^{-j\omega\tau} d\tau$$

(4.31)

The first term of (4.31) is[4-19]:

$$(Ap + Bq)^2 \frac{1}{2\pi} \int_{-\infty}^{\infty} e^{-j\omega\tau} d\tau = (Ap + Bq)^2 \delta(\omega)$$

(4.32)

where the expression given by the integral is the delta function $\delta(\omega)$, and represents the power of the d.c. current component. For the second term of (4.31) we may drop $|\tau|$ for τ and write:

$$\frac{(A-B)^2 pq}{\pi} \, \text{Re} \int_{0}^{\infty} e^{-(\mu+\eta)\tau} e^{-j\omega\tau} d\tau = \frac{(A-B)^2 pq}{\pi} \frac{(\mu+\eta)}{(\mu+\eta)^2 + \omega^2}$$

(4.33)

where Re means the real part.

Hence, the power density spectrum of Fig. 4.4 is given by:

$$S(\omega) = (Ap + Bq)^2 \delta(\omega) + \frac{(A-B)^2 pq}{\pi} \frac{(\mu+\eta)}{(\mu+\eta)^2 + \omega^2}$$

(4.34)

4.2 Spectrum of Burst Noise with Flicker Noise Superimposed

From the observation of burst noise in transistors we have seen that there is a superimposed signal of noise $\phi(t)$ on the noise current pulses $f(t)$. Hence in Fig. 4.3 the total noise signal $F(t)$ is made up of $f(t)$ and $\phi(t)$.

The flicker noise-power density component is known experimentally to be of the type

$$S_F(\omega) = H \, I^2 \, \omega^{-\beta}$$

(4.35)

where H is a constant, I is the d.c. current and the parameter β is usually near to 1. Since the power density of the flicker noise is proportional to I^2, the flicker noise current is proportional to

86

the d.c. current. Hence, the amount of flicker noise at levels A
and B is proportional to these levels respectively. Consequently,
assuming that the superimposed noise signal $\phi(t)$ at a d.c. current
of 1 A corresponds to the flicker noise, the noise signal $F(t)$ in
Fig. 4.3 is expressed by:

$$F(t) = f(t) + f(t) \cdot \phi(t) = f(t) (1 + \phi(t)) \qquad (4.36)$$

The autocorrelation function of $F(t)$ is given by:

$$R(\tau) = \overline{f(t) (1 + \phi(t)) \cdot f(t+\tau) (1 + \phi(t+\tau))} = \overline{f(t)f(t+\tau)} \cdot$$

$$\overline{(1 + \phi(t) + \phi(t+\tau) + \phi(t)\phi(t+\tau))} \qquad (4.37)$$

We assume that the generation process of the burst noise is inde-
pendent of the generation process of the flicker noise. This assump-
tion is based on the experimental fact that sometimes only one of
the two types of noise is present, while at other times both take
place; but even then they may appear at different spectrum ranges.
These considerations allow us to write (4.37) as:

$$R(\tau) = \overline{f(t) \ f(t+\tau)} \cdot (1 + \overline{\phi(t)\phi(t+\tau)}) = R_B(\tau) (1 + R_\phi(\tau)) \quad (4.38)$$

where $R_B(\tau)$ and $R_\phi(\tau)$ are the autocorrelation functions of the burst
noise and of the flicker noise for unity current respectively.

The noise-power density spectrum as given by (4.30) is:

$$S(\omega) = \frac{1}{2\pi} \int_{-\infty}^{\infty} (R_B(\tau) + R_B(\tau)R\phi(\tau)) \ e^{-j\omega\tau} d\tau \qquad (4.39)$$

The first term of the right-hand side of (4.39) gives the power den-
sity spectrum of the burst noise $S_B(\omega)$ which is known through equa-
tion (4.34). Let us calculate the second term:

$$\frac{1}{2\pi} \int_{-\infty}^{\infty} R_B(\tau)R_\phi(\tau) \ e^{-j\omega\tau} d\tau \qquad (4.40)$$

Having substituted $R_B(\tau)$ given by (4.27) we obtain:

$$(Ap + Bq)^2 \frac{1}{2\pi} \int_{-\infty}^{\infty} R_\phi(\tau) \, e^{-j\omega\tau} d\tau + (A-B)^2 p \, q \, \frac{1}{2\pi} \int_{-\infty}^{\infty} \left[R_\phi(\tau) \right.$$
$$\left. e^{-(\mu+\eta)|\tau|} \right] e^{-j\omega\tau} d\tau \qquad (4.41)$$

Now, the first term in (4.1) is the power density spectrum of the flicker noise $S_F(\omega)$, (Ap + Bq) being the d.c. current. Therefore, through (4.35) the first term is:

$$S_F(\omega) = (Ap+Bq)^2 \frac{1}{2\pi} \int_{-\infty}^{\infty} R_\phi(\tau) e^{-j\omega\tau} d\tau = (Ap+Bq)^2 H \, \omega^{-\beta} \qquad (4.42)$$

The second term of (4.41) is the power density spectrum of the cross component burst-flicker, $S_{BF}(\omega)$, or the cross power spectrum. The integral of the second term is of the same order of magnitude as the integral of the first term; hence, their ratio is of the order of magnitude of $(A-B)^2 pq/(Ap+Bq)^2$. Thus the contribution of $S_{BF}(\omega)$ to the total spectrum is negligible.

Therefore, the noise power density spectrum of Fig. 4.3 is obtained by substituting in (4.39) the values calculated through equations (4.34) and (4.42), having neglected the cross term $S_{BF}(\omega)$. The total spectrum $S(\omega)$ is given by:

$$S(\omega) = (Ap + Bq)^2 \delta(\omega) + \frac{(A-B)^2 pq}{\pi} \frac{(\mu+\eta)}{(\mu+\eta)^2 + \omega^2} + \frac{(Ap+Bq)^2 H}{\omega^\beta} \qquad (4.43)$$

which agrees well with equation (1.10).

5. Measurements of Burst Noise in Transistors

The first time we came across the burst noise in transistors was during the design and construction of the pre-amplifier and of the very low frequency filter (Chapter 3, sections 3 and 5). Since then, our interest in this noise phenomenon has continued to increase especially with respect to bursts of very low frequency.

We have observed in transistors burst noise over 7 decades of frequency, 10^{-3} to 10^4 Hz. In general, in any transistor we have ob-

88

served that the phenomenon extends over approximately 3 decades
within the above limits. Im comparison with the low frequency noise
of carbon resistors there is one significant difference. The measured
noise power density value can in general be repreated with $\pm$ 2ε sta-
tistical error for the measuring time T. Only very seldom could the
measurement not be repeated with the desired accuracy, a fact that
agrees with the slight variation of the variance of noise that has
been found in semiconductors and transistors[4-16]. Thus, in practice
the random process of burst noise in transistors is a stationary one.

After a tedious observation of the burst noise in transistors the
pulse lenghts showed a clear Poisson probability distribution. In
the frequency range of its appearence the noise power density spec-
trum follows an f^{-2} law when the burst noise component is larger
than the flicker noise component. Such is assumed to be the situa-
tion of the noisy transistors we have chosen for measurement.

It has been particularly difficult to choose the measuring samples.
Sometimes, one difficulty arises from the simultaneous presence of
more than two levels of noise, even four levels being not rare, re-
sulting in two, three or four series of pulses with different am-
plitudes among themselves but constant for each series. Another dif-
ficulty is that each series may have a different frequency range of
pulses yielding a spectrum with more than one "bump". On rare occa-
sions a sample had a random switching "on" and "off" of the pulse
series, while in other samples the burst noise could be started or
stopped by varying the collector voltage. Finally, it was equally
difficult to find samples which, apart from having only one series
of noise pulses, had a mean pulse length detectable inside the fre-
quency range of the measuring channel (10^{-2} to 20 Hz).

Among 30 bipolar transistors with burst noise we have found 3 to
which the above difficulties do not apply and are therefore measur-
able in accord to our needs and means. Two samples are npn transis-
tors and the third one is a pnp type. All three are operated at a
collector current of approximately 2 μA, giving output burst pulses
from 400 μV max. to 100 μV max. amplitude across a resistor load
(Chapter 3, section 2).   **89**

Fig. 4.5   Relative magnitude of the noise power density spectrum
            ω.S(ω) of a transistor, with very-low frequency burst
            noise present. Estimated curve of S(ω)

Fig. 4.6   Relative magnitude of the noise power density spectrum
ω.S(ω) of a transistor, with very-low frequency burst
noise present. Estimated curve of S(ω)
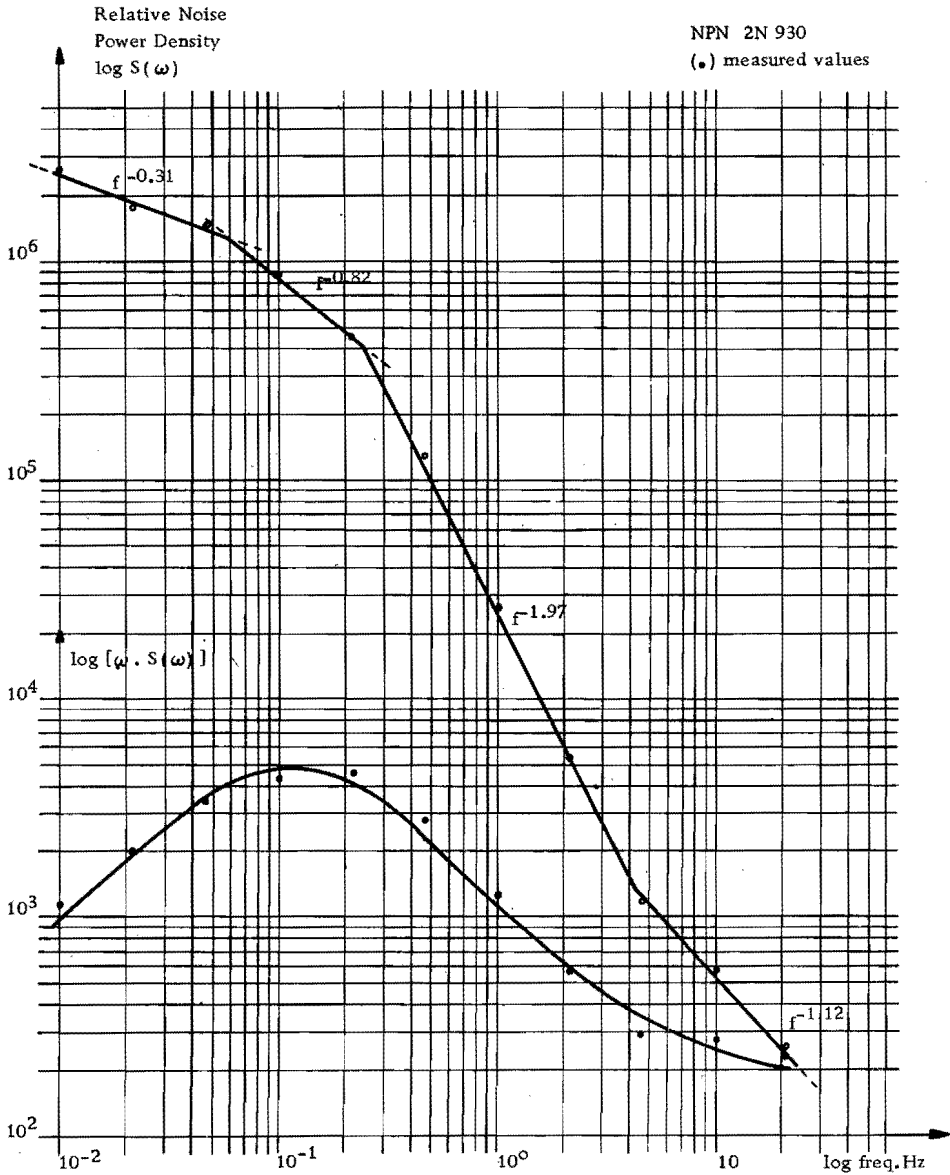
Fig. 4.7   Relative magnitude of the noise power density spectrum
            $\omega \cdot S(\omega)$ of a transistor, with very-low frequency burst
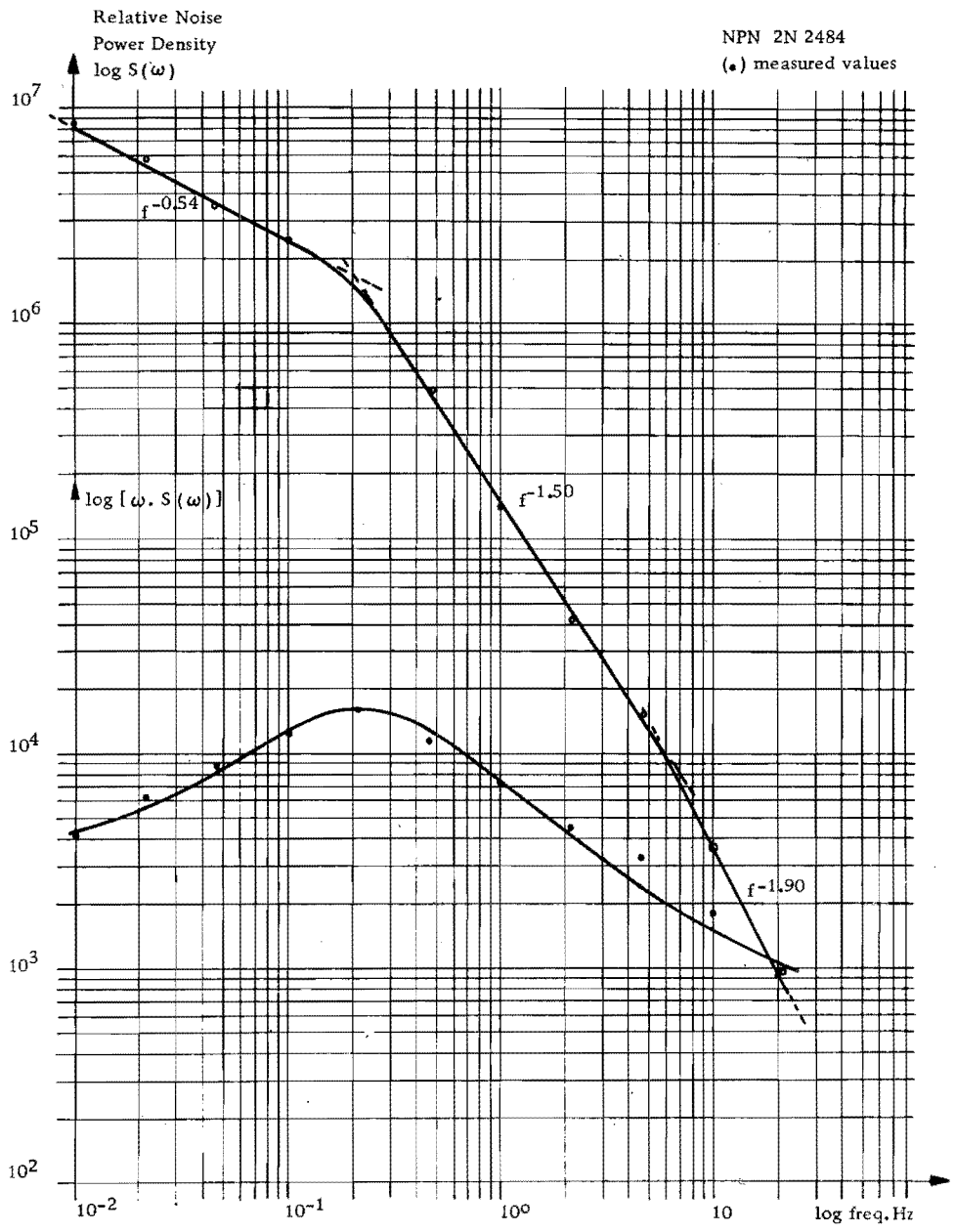   noise present. Estimated curve of $S(\omega)$

Owing to the prewhitening filter the measured values correspond to $\omega \cdot S(\omega)$ for each transistor under investigation.

Figs. 4.5, 4.6, and 4.7 represent the relative magnitude of the $\omega \cdot S(\omega)$ spectrum for the three transistors. This spectrum was measured with an ε of 2% for the frequencies of 20 and 10 Hz, an ε of 5% for the frequencies down to $2.15 \cdot 10^{-2}$ Hz, and of 7.5% for the 10^{-2} Hz.

Each graph shows a clear bump around the mean burst frequency f_b, which has been observed on the oscilloscope. The burst noise component appears clearly in Figs. 4.5 and 4.6, while in Fig. 4.7 the flicker noise component is prominent.

Each graph has been recoloured i.e. the ordinates have been divided by ω and drawn in the same figure to obtain a relative magnitude curve of the real input spectrum $S(\omega)$. The new curve is approximated by straight line sections and made to pass through an arbitrarily chosen point.

The recoloured curve approximates well the curve of Fig. 4.8, where arbitrary flicker and burst noise components are shown. In fact, log $S(\omega)$ of Fig. 4.5 can be made to correspond to the NPQR section of Fig. 4.8, while log $S(\omega)$ of Figs. 4.6 and 4.7 would correspond to the NPQ and MNPQ sections, respectively, in Fig. 4.8.
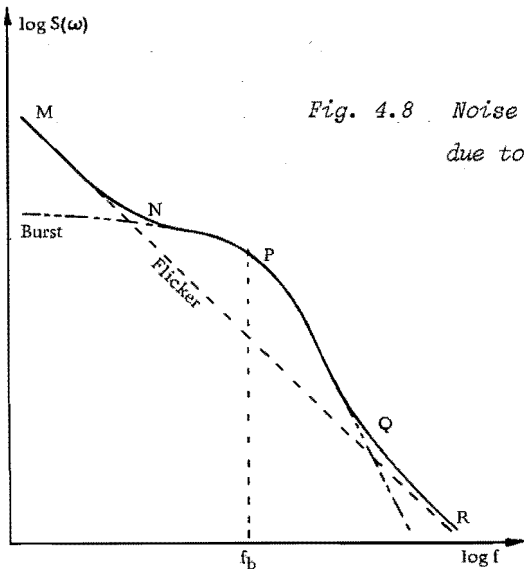
Fig. 4.8 *Noise power density spectrum $S(\omega)$ due to burst noise and flicker noise*

Owing to the input d.c. blocking capacitor of the measuring channel
the first term in the right-hand side of equation (4.43) is suppress-
ed in the measurement. Taking into consideration the prewhitening ac-
tion, we obtain, at the output of the channel the noise power density
spectrum $\omega \cdot S(\omega)$, given by:

$$\omega \cdot S(\omega) = \frac{(A-B)^2 pq}{\pi} \; \frac{(\mu+\eta)\;\omega}{(\mu+\eta)^2+\omega^2} + \frac{(Ap+Bq)^2 H \;\omega}{\omega^\beta} \qquad (4.44)$$

The best fit of the experimental values to equation (4.44) is obtain-
ed by means of a computer programme of the last squares method. The
computerised parameter values are the following:

	$(A-B)^2 pq/\pi$	$(Ap+Bq)^2 H/(\mu+\eta)^{\beta-1}$	$(\mu+\eta)$	$\beta-1$
$\omega \cdot S(\omega)_{4.5}$:	9696	100	0.109	−0.075
$\omega \cdot S(\omega)_{4.6}$:	29438	1762	0.22	+0.18
$\omega \cdot S(\omega)_{4.7}$:	169	71	14	+0.34

The computerised values of $\omega \cdot S(\omega)$ for the above parameters are plot-
ted on a curve in their corresponding figures and the experimental
values are seen to follow equation (4.44). Hence, we have obtained an
estimated value of the exponent β of the flicker noise component and
we may conclude that equation (4.43) represents the noise power den-
sity spectrum of an electronic device in which flicker and burst noise
are simultaneously present as illustrated by Fig. 4.3.

94

SUMMARY

The present thesis deals with very-low frequency spectra of the e-
lectrical noise in carbon film resistors and in bipolar planar tran-
sistors.

The basic knowledge required to approach the study of noise is intro-
duced in chapter I by considering the properties of random phenomena.
The fluctuations of electrons give rise to electrical noise, the pow-
er spectrum of which is considered especially at very low frequencies.
In this frequency range, the flicker noise and the burst noise are
the main noise components, which are a function of the frequency (ω)
to some power $-\beta$.

Flicker noise is ubiquitous and its anomalous behaviour is exposed
by considering the deviations of the value of β from unity in the
noise power density spectrum $S(\omega)$.

Burst noise appears to be more sporadic in nature and its waveform
is seen to be of a more defined type as of an unsymmetrical random
telegraph signal. The value of the exponent β is close to 2.

The theoretical basis for measuring noise power spectra is presented
in chapter II. Through the considerations made on the autocorrela-
tion function of a noisy signal and the introduction of a spectral
window we arrive at a theoretical measuring system for power spectra.

The importance of a low Q frequency window and of the prewhitening
action is emphasised, while attention has been given to the neces-
sary measuring time for the desired statistical accuracy. The fre-
quency band was selected by changing the capacitors thus keeping the
same noise producing elements in the circuit. The difficulty of meas-
uring very-low frequency voltages is solved by the hybrid approach
of an analogue-to-digital converter.

95

The realisation of an actual measuring channel for power spectra is presented in detail in chapter III. The first six blocks have been designed and constructed. The main ones among them are the pre-amplifier, the wide-band prewhitening filter and the selective amplifier. The pre-amplifier is operated in a hushed-mode yielding a low drift, low noise and low distortion performance. The first two differential stages are based on an improved collector-source current which consists of a compound transistor pnp-npn with an input base current in the nanoampere range. The linearity of the prewhitening filter is excellent and allows an easy recolouring of the power spectra at the output of the channel. Owing to the wiring complexity of the Twin-T circuit necessary for the selective amplifier, the required frequency compensation is obtained by a practical procedure. In the first few blocks it was essential to avoid the presence of burst noise in all transistors and to find some very well matched transistor pairs. The construction of these blocks required first-class components and a careful lay-out.

The noise power measurements obtained from carbon film resistors and planar bipolar transistors within the range of 10^{-2} to 20 Hz are shown in chapter IV. By repeating noise power measurements during the same length of time on the same carbon resistor we have found that the flicker noise of some carbon resistors is a quasi-stationary random process.

The cause of this quasi-stationarity is thought to be found in the observed random bursts that change the noise excitation state of the carbon resistor. One and the same sample gave a spread from 0.8 to 1.6 in the value of β, which agrees with the spread found by most experimenters (chapter IV, table I) on different samples and frequency ranges. This fact helps to understand the difficulty encountered when repeating low-frequency noise measurements.

With respect to burst noise we have derived two expressions. The first is the mathematical expression of the noise power density spectrum of an unsymmetrical random telegraph signal between two levels. Secondly, considering that the flicker noise voltage is superimposed on the burst noise voltage and is proportional to the d.c. level of

the burst signal, an expression has been obtained for the noise spectrum $S(\omega)$ when flicker and burst noise are simultaneously present.

We have measured the noise spectrum of transistors that showed to have burst noise in the frequency range given above, and have found that the spectrum follows the calculated expression.

REFERENCES

Chapter I

1-1   Diogène Laërce. Vies des Plus Illustres Philosophes Grecs de
              l'Antiquité. Traduites du grec. Vol. I. 250 a.c.

1-2   Stoney, G.J. "On the cause of double lines and equidistant
              satellites in spectra gases". Scit.Trans.Roy.
              Dublin Soct. 1891. July.

1-3   Brown, R. "On the existence of active molecules in organic and
              inorganic bodies". Phil.Mag. 1828, Vol.4, Sept.
              pp. 161-173.

1-4   Bendat, J.S.;Piersol, A.G. Measurement and Analysis of Random
              Data. John Wiley. 1966, p.12.

1-5   Nyquist, H. "Thermal agitation of electric charge in conductors".
              Phys.Review. 1928. Vol. 32, p. 110-13.

1-6   Bull, C.S. Fluctuations of Stationary and Non-Stationary Elec-
              tron Currents. Butterworths. 1966, p. 66.

1-7   Van der Ziel, A. Noise. Prentice Hall. 1954, p.31.

1-8   Brophy, J. Basic Electronics for Scientists. McGraw-Hill. 1966,
              p.269.

1-9   Bloodworth, G.G.;Hawkins, R.J. "The physical basis of current
              noise" Radio and Electro.Eng. 1969. Vol. 38,
              July. p. 17.

1-10 Johnson, J.B. "The Schottky effect in low frequency circuits".
              Phys.Review. 1925. Vol. 26, p. 71-85.

1-11 Bernamont, J. "Fluctuations de résistance dans un conducteur
              métallique de faible volume". Compt.Rd. 1934.
              Vol. 198, pp. 2144-6.

1-12 Meyer, E.;Thiede, H. "Resistance fluctuations in thin carbon
        films". (In German) E.N.T. 1935. Vol. 12, pp.
        237-42.

1-13 Christensen, C.J.;Pearson, G.L. "Spontaneous resistance fluc-
        tuations in carbon microphones and other gran-
        ular resistances". Bell.Syt.Tech.J. 1936. Vol.
        15, pp. 197-223.

1-14 Van Vliet, K.M.;Van Leeuwen, C.J.;Blok, J.;Ris, C. "Measure-
        ments on current noise in carbon resistors and
        in thermistors". Physica. 1954. Vol. XX, pp.
        481-96.

1-15 Fonger, W.W. "A determination of 1/f noise sources in semi-
        conductor diodes and triodes". Transistor I.
        1956. pp. 239-295.

1-16 Van Vliet, K.M. "Noise in semiconductors and photoconductors".
        Proc. IRE. 1958, June. pp. 1004-1018.

1-17 Attkinson, W.R.;Frey, L.;Newman, J. "Spectrum analysis of ex-
        tremely low frequency variations of quartz os-
        cillators". Proc. IEEE. 1963. Vol. 51, p. 379.

1-18 Mansour, I.R.M.;Hawkins, R.J.;Bloodworth, G.G. "Measurements
        of current noise in mos transistors from 5.10^{-5}
        to 1 Hz". Radio and Electro. Eng. 1968. April.
        pp. 212-216.

1-19 Malakof, A.N. "The problem of the flicker noise spectrum". (In
        Russian) Radiotecknika and Electronika. 1959.
        Vol. 4, pp. 54-62.

1-20 Van der Ziel, A. "Low frequency noise in vacuum tubes", in
        Noise in Electron Devices. Edt.Smullin-Haus.
        John Wiley, 1959. p. 67.

1-21 Kleyner, E.Yu,;Amiryan, R.A.; Vorob'yev, M.D. "Anomalous flick-
        er noise in tubes with oxide cathodes". Radio
        Eng. and Electro.Phy. 1969. Vol. 14,
        pp. 636-38.

1-22 Vasseur, J.P. Propriétés et Applications des Transistors. Soc.
                    Fran. de Docum.Electro.Paris. 1958. p. 450.

1-23 Van der Ziel, A. do. 1-7, p. 206.

1-24 Bess, L.;Kisner, L.S. "Investigation of 1/f noise spectra".
                    Jour.App.Phy. 1966. Vol. 37. Augt. pp.3458-62.

1-25 Fetina, V.N. "Anomalies in the low frequency noise fluctuations
                    observed in narrow germanium p-n junctions".
                    Radio Eng. and Electro.Phy. 1966. Vol. 11.
                    Sept. pp. 1444-48.

1-26 Verster, T.C. "Anomalies in transistor low-frequency noise".
                    Proc. IEEE. 1967. Vol. 55. July. pp. 1204-5.

1-27 Nakahara, M; Iwasawa, H; and Yasutake, K. "Anomalous low-fre-
                    quency noise enchancement beyond pinch-off in
                    silicon n-channel mos transistors".
                    Proc. IEEE. 1969. Vol. 57. Dec. pp. 2177-78.

1-28 Campbell, R.H.; Chipman, R.A. "Noise from current-carrying
                    resistors 20 to 500 Kc". Proc. IRE. Waves and
                    Electrons Sect. 1949. Augt. pp. 938-42.

1-29 Oakes, F. "The measurement of noise in resistors". Electro.
                    Eng. 1950. Nov. pp. 464-69.

1-30 Kirby, P.L. "Current noise in fixed carbon resistors", in
                    Noise in Electronic Devices. Chapman and Hall.
                    1961. pp. 78-85.

1-31 Pay, R.G.; given by Bell, D.A. Electrical Noise. Van Nostrand.
                    1960. p. 262.

1-32 Minden, H.T. "Noise behaviour of avalanche silicon diodes".
                    Proc. IEEE. 1966. Vol. 54. Augt. pp. 1124-25.

1-33 Card, W.H.;Chaudhari, P.K. "Characteristics of burst noise".
                    Proc. IEEE. 1965. Vol. 53. June. pp. 652-53.

1-34 Wolf, D.; Holler, E. "Bistable current fluctuations in reverse-
                    biased p-n junctions of germanium". Jour.App.
                    Phy. 1967. Vol. 38. Jan. pp. 189-92.

1-35 Giralt, G.;Martin, J.C.;Mateu-Perez, F.X. "Sur un phenomène
            de bruit dans les transistors, caracterisé par
            des créneaux de courant d'amplitude constante".
            Comt. Rd. Acd. Sc. Paris. 1965. Group V. pp.
            5350-5353.

1-36 Giralt, G.;Martin, J.C.;Mateu-Perez, F.X. "Le bruit en créneaux
            des transistors plans au silicium". Electronic
            Letters. 1966. June. Vol. 2. pp. 228-29.

1-37 Martin, J.C.;Mateu-Perez, F.X.;Serra-Martin, F. "Mesures du
            bruit de fond des transistors plans aux très
            basses fréquences". Electronic Letters. 1966.
            Sept. pp. 343-345.

1-38 Hsu, S.T.;Whittier, R.J. "Characterization of burst noise in
            silicon devices". Solid-St.Elect. 1969. Vol.
            12. Nov. pp. 868-78.

1-39 Widlar, R. "What is popcorn noise". Electro.Design.1968. No.
            11. p. 88.

1-40 Smith, L.;Sheingold, D.H. "Noise and operational amplifier
            circuits". Analogue Dialogue. 1969. March. p.9.

1-41 Leonard, P.L.;Jaskolski, S.V. "An investigation into the ori-
            gin and nature of popcorn noise". Proc. IEEE.
            1969. Vol. 57. Oct. pp. 1786-88.

Chapter II

2-1   Lee, Y.W. Statistical Theory of Communication. John Wiley.
            1960. p. 329.

2-2   Lee, Y.W. do.   p. 332.

2-3   Blackman, R.B.;Tukey, J.W. The Measurement of Power Spectra.
            Dover 1959. p. 70.

2-4   Blackman, R.B.;Tukey, J.W. do.   p. 100.

2-5   Bendat, J.S.;Piersol, A.G. Measurement and Analysis of Random
            Data. John Wiley 1966. p. 269.

2-6   Bendat, J.S.;Piersol, A.G. do.   p. 199.

2-7   Bendat, J.S.;Piersol, A.G. do.   p. 261.

2-8   Richards, P.I. "Computing reliable power spectra", Spectrum
                IEEE. 1967. Jan. pp. 83-90.

2-9   Bull, C.S. Fluctuations of Stationary and Non-Stationary Elec-
                tron Currents. Butterworth. 1966. p. 160.

Chapter III

3-1   Volkers, W.K.;Pederson, N.E. "The hushed transistor amplifier".
                Teletech. and Electronic Indust.:Part I, 1955.
                Dec. p. 82. Pt. II, 1956. Jan. p. 70. Pt. III,
                1956. Feb. p. 72.

3-2   Owens, A.R.;Perry, M.A. "Low current amplifier using silicon
                planar transistors". Proc. IEE. 1965. vol. 112,
                Nov. p. 2005.

3-3   Chappell, A.D. "Effect to collector voltage and collector cur-
                rent on junction temperature". Elect.Letters.
                1965, Nov. p. 259.

3-4   Müller, O. "Thermal feedback and 1/f noise in transistors".
                1965 Internat.Solid St.Cirt.Conf. p. 68-69.

3-5   Reid, F.A. "Dynamic thermal response and voltage feedback in
                junction transistors". IBM-Journal. 1966. Jan.
                p. 95-97.

3-6   Herbst, L.J. "D.C. differential amplifier with very high com-
                mon-mode rejection". Elect. Letters. 1965. March.
                p. 41.

3-7   Reynolds, J. "Nonlinear distortions and their cancelations in
                transistors". IEEE Trans. Electron Devices.
                Vol. ED-12. 1965. Nov. p. 595-99.

3-8   Baxandall, P.J.;Shallow, E.W. "Constant current source with
                unusually high internal resistance and good
                temperature stability". Electr. Letters. 1966.
                Sept. p. 351.

102

3-9   Bhola, S.K.;Murphy, R.H. "Low drift design of differential am-
                plifiers". Electron.Eng. 1966. Oct. p. 659-61.

3-10   Pinto, J.J. "Transistor low drift d.c. amplifiers". Electron.
                Eng. 1964. May. p. 304-308.

3-11   Hoffait, A.H.;Thornton, R.P. "Limitations of transistor d.c.
                amplifier". Proc. IEEE. 1964. Feb. p. 179.

3-12   Thornton, R.P. et alii. "Multistage Transistor Circuits". J.
                Wiley. 1965 SEEC vol. 5. p. 220.

3-13   Widlar, R.J. "An exact expression for the thermal variations
                of the emitter-base voltage of bipolar transis-
                tors". Proc. IEEE. 1967. Jan. p. 97.

3-14   Owens, A.R.;Jones, J.M. "Low-current operation of silicon pla-
                nar transistors". Electron. Letters. 1965. Oct.
                n° 8. p. 242-3.

3-15   Chaplin, G.B.B. "D.C. amplifiers". Handbook of Semiconductor
                Electronics. Hunter. McGraw Hill. 1962. p. 13-3.

3-16   Bartolomew, C.Y. "Analysis of transistor I_{CBO} excess currents
                by gamma irradiation". IEEE Trans.Elect.Dev.
                1969. Jan. pp. 153-4.

3-17   Hsu, S.T.;Whitter, R.J. "Characteristics of burst noise in si-
                licon devices". Solid State Elect. 1969. Vol.
                12. Nov. p. 869.

3-18   Cowles, L.G. Analysis and Design of Transistor Circuits. Van
                Nostrand. 1966. p. 25.

3-19   Baxandall, P.J.;Shallow, E.W. "Constant-current source with
                unusually high internal resistance and good tem-
                perature stability". Electr. Letters. 1966.
                Sept. 1966. n° 9. p. 351-52.

3-20   Nielson, E.G. "Behaviour of noise figure in junction transis-
                tors" Procd. IRE. 1957. Vol. 45. p. 957-63.

3-21   Rheinfelder, W.A. "Design of Low-Noise Transistor Input Cir-
                cuits". Hayden. 1964. p. 13.

3-22 Faulkner, E.A.;Grimbley, J.B. "Reduction of flicker noise in
transistor amplifiers". Electr. Letters. 1968.
Vol. 4. n⁰ 5. p. 80-81.

3-23 Hurley, R.B. "Junction Transistor Electronics". Wiley, 1958.
p. 110-112.

3-24 Lotsch, K.V. "Nonlinear distortions and their cancellation in
transistors". IEEE Trans. E-D. 1966. June. pp.
532-33.

3-25 Reynolds, J.;Khy, T.L. "Elimination of intermodulation in
transistors". Proceed. IEEE. 1966. May. pp.801.

3-26 Navarro Borrás, F.;Rios, S. Analisis Matemético. Edt.Stylos.
Madrid. 1944. p. 474.

3-27 Moll, J.L. "The evolution of the theory for the voltage-cur-
rent characteristic of p-n junctions". Proc.
IRE. 1958. June. p. 1072-82.

3-28 Holmes, P.J. "Transistor abnormalities as revealed by current-
voltage characteristics". Radio and Elect.Eng.
1969. vol. 38. n⁰ 5. Nov. p. 257.

3-29 Zaalberg van Zelst, J.J. "Calculations of impedances the phase-
angle of which lies between prescribed values
in a certain frequency range". (In Dutch) Phi-
lips Nat. Lab, 1961. Report No. 63/61.

3-30 Horowitz, I.M. "Exact design of transistor RC band-pass fil-
ters with prescribed active parameter insensi-
tivity". IRE Trans. Cirt Theory. 1960. Sept.
p. 313-320.

3-31 Klein, G.;Zaalberg van Zelst, J.J. "Precision Electronics".
Philips Tech.Lib. 1967. p. 258.

3-32 Cowles, L.G. "The parallel-T R-C network". Procd. IRE. vol.
40. 1952. Dec. p. 1712-17.

3-33 Valley, G.E.;Wallman, H. "Vacuum Tube Amplifiers". McGraw.
1948. p. 394.

104

3-24 Hurley, R.B.   do. 3-23, p. 101.

3-35 Murari, B. "Thermal drift in ultra low drift amplifiers".
                Procd. IEEE. 1965. May. p. 556.

3-36 Handbook of Operational Amplifier.Active RC Networks. Burr-
                Brown 1966. p. 74.

Chapter IV

4-1   Bernamont, J. "Fluctuations de résistance dans un conducteur
                métallique de faible volume". Comt.Rd.Acad.Sci.
                1934, vol. 198, pp. 1755-58.

4-2   Otto, R. "Noise in carbon microphone" (In German). Hochfreq.U.
                Elekt.Akust. 1935, vol. 45, pp. 187-98.

4-3   Meyer, E;and Theide, H. "Resistance fluctuations in thin car-
                bon films" (In German). E.N.T. 1935, vol. 12,
                pp. 237-42.

4-4   Christensen, C.J.;and Pearson, G.L. "Spontaneous resistance
                fluctuations in carbon microphones and other
                granular resistances". Bell Syst.Tech.J. 1936,
                vol. 15, pp. 197-223.

4-5   Abson, E.J.;Harris, W.;and Roberts, W.L. "Semiconductor-noise
                at low frequencies". T.R.E. 1946. Report 2051.
                22nd-Nov.

4-5   Campbell, R.H.;and Chipman, R.A. "Noise from current carrying
                resistors 20 to 500 Kc". Proc.I.R.E. 1949, vol.
                37, pp. 938-42.

4-7   Templeton, I.M.;and MacDonald, D.K.C. "The electrical conduc-
                tivity and current noise of carbon resistors".
                Proc.Phys.Soc.B. 1953, vol. 66, p. 680.

4-8   Van Vliet, K.M.;Van Leeuwen, C.J.;Block, J. and Ris, C. "Meas-
                urements on current noise in carbon resistors
                and in thermistors". Physica. 1954, vol. 20,
                pp. 481-96.

4-9   Kirby, P.L. "Current noise in fixed carbon resistors", in
              Noise in Electronic Devices. Chapman and Hall.
              1961, pp. 78-85.

4-10 Brophy, J.J. Basic Electronics for Scientists. McGraw-Hill,
              1966, p. 271.

4-11 Williams, J.L.;and Burdett, R.K. "Current noise in cermet
              resistor films". Brit.J.Appl.Phys. 1966, vol.
              17, pp. 977-78.

4-12 Mandelbrot, B. "Some noises with 1/f spectrum, a bridge between
              direct current and white noise". IEEE trans.
              1967, I-T-13, pp. 289-98.

4-13 López de la Fuente, J. "Quasi-stationary noise in resistors".
              Electronics Letters. 1969, vol. 5, n° 12, pp.
              63-5.

4-14 Malakof, A.N. "The problem of the flicker-noise spectrum" (In
              Russian). Radioteck. and Electro. 1959, vol. 4,
              Jan. p. 59.

4-15 Brophy, J.J. "Statistics of 1/f noise". Phy.Review. 1968, vol.
              166, n° 3, pp. 827-31.

4-16 Brophy, J.J. "Variance fluctuations in flicker noise and cur-
              rent noise". Journ.Appl.Phys. 1969, vol. 40,
              n° 9, p. 3553.

4-17 Radeka, V. "1/f noise in physical measurements". IEEE trans.
              1969, N-Sc. vol. 16. Oct. p. 29.

4-18 Kenrick, G.W. "The analysis of irregular motions with appli-
              cations to the energy-frequency spectrum of
              static and telegraph signals". Phil.Mag.Ser.7.
              1929, vol. 7, pp. 176-96.

4-19 Lee, Y.W. Statistical Theory of Communication. J. Wiley, 1960,
              p. 49.

106

AKNOWLEDGEMENTS

CURRICULUM VITAE

7th November, 1927 : Born at Neguri-Guecho, Vizcaya, Spain

1934 : Grammar studies at the preparatory school of
St. Edmund's College, Ware, England

1938 : Grammar School studies at the Sacred Heart
High School, Vitoria, Spain

July, 1946 : University Baccalaureate (B.U.),
University of Valladolid, Spain

October, 1946 : Studies of mathematics
Academia Luz, Madrid, Spain

October, 1951 : Joined the Society of Jesus (S.J.)

July, 1957 : Licentiate in Philosophy (Ph.L.),
Catholic University of Quito, Ecuador

June, 1961 : Master of Science (Research) in Electrical
Engineering (M.Sc.), St. Louis University,
St. Louis, Mo. U.S.A.

August, 1964 : Priesthood, Brussels, Belgium

July, 1965 : Licentiate in Theology (Th.L.)
Collège St. Albert, Louvain, Belgium

October, 1965 : Started research work in the Electronics Group
of the Electrical Engineering Department of
the Eindhoven University of Technology, Nether-
lands.

STELLINGEN - PROPOSITIONS

The noise of some carbon resistors at very-low frequencies is gener-
ated by a quasi-stationary random process.
Thesis. Sect. 4.2, 4.3.

II

Even at very-low frequencies the burst noise component of the noise
in planar bipolar transistors can be larger than the flicker noise
component yielding at least one bump in the spectrum curve.
Thesis. Sect. 4.4.2, 4.5.

III

The expression of the power spectrum of a random telegraph wave is
given in the literature [1] for the situation of a symmetrical wave.
Measurements of burst noise [2] are compared with such an expression.
In general, such a procedure is not correct since the wave is un-
symmetrical and a new expression is needed.
Thesis. Sect. 4.4.1, 4.5.

1. Lee, Y.W. Statistical Theory of Communication. J. Wiley, 1960,
            p. 221.
2. Jeager, R.C.; Brodersen, A.J. "Low-frequency noise sources in bi-
            polar junction transistors". IEEE.Trans.E.D.-17, 1970,
            p. 131.

IV

Modern scientific researchers should acquire a sufficient understan-
ding of numerical analysis since by means of numerical methods digit-
al computers have become a significant and universal instrument for
solving broad classes of problems.

V

Man must be educated through arts and sciences as a whole being, so
that he obtains a broad background education and a deep specialisa-
tion in some field. Thus a graduated scholar in liberal arts is not
more fully educated than a professional graduated from a science de-
partment.

VI

The christian believer and scientific researcher may reach a total development of his personality by discovering the intelligence of nature as established by God in favour of mankind.
"L'analyse de la Matière révèle à qui sait voir, la priorité, la primauté de l'Esprit".
Teilhard de Chardin. Science et Christ. Ed.Seiul,Paris. 1965, p.57.

VII

The scientist and the engineer of to-day are anxious of learning and knowing about the ideas of others engaged in the same field in other countries. Hence, the learning of technical foreign languages is compulsory and may be very much aided by following technical courses taught in foreign languages.

VIII

The freshman student of engineering should be given some motivation and feeling for the need of mathematics and physics by means of guided experiments in his own desired future field. This experimental procedure can help the student to decide at the end of his first scholar year whether or not he should continue with technical studies without the need of having to take an entrance examination.

IX

Technical education at its medium level should be given in close coordination with the actual industrialisation of products and methods.

X

The technical institutions of developed countries have a moral obligation to help their homologous institutions of underdeveloped countries to acquire a better technical knowledge.

Eindhoven, 30 juni 1970   Julio López de la Fuente